2145-33

Spring College on Computational Nanoscience

17 - 28 May 2010

Nanostructured Carbon and Complex Oxides

Risto NIEMINEN

COMP/Applied Physics
Aalto University School of Sciences & Technology
Espoo
Finland

Spring College in Computational Nanoscience
Trieste, May 17-28, 2010

Aalto University

Computational nanoscience: carbon nanostructures, complex oxides

Risto Nieminen

COMP/Applied Physics
Aalto University School of Science and Technology

1. Transport in functionalised nanotubes
   (Javad Hashemi, poster)

2. Magnetic impurities in graphene

3. Complex oxides:
   - perovskite interfaces and superlattices
     (Riku Oja, poster)
   - defects in transparent conducting oxides

CARBON NANOBUDS

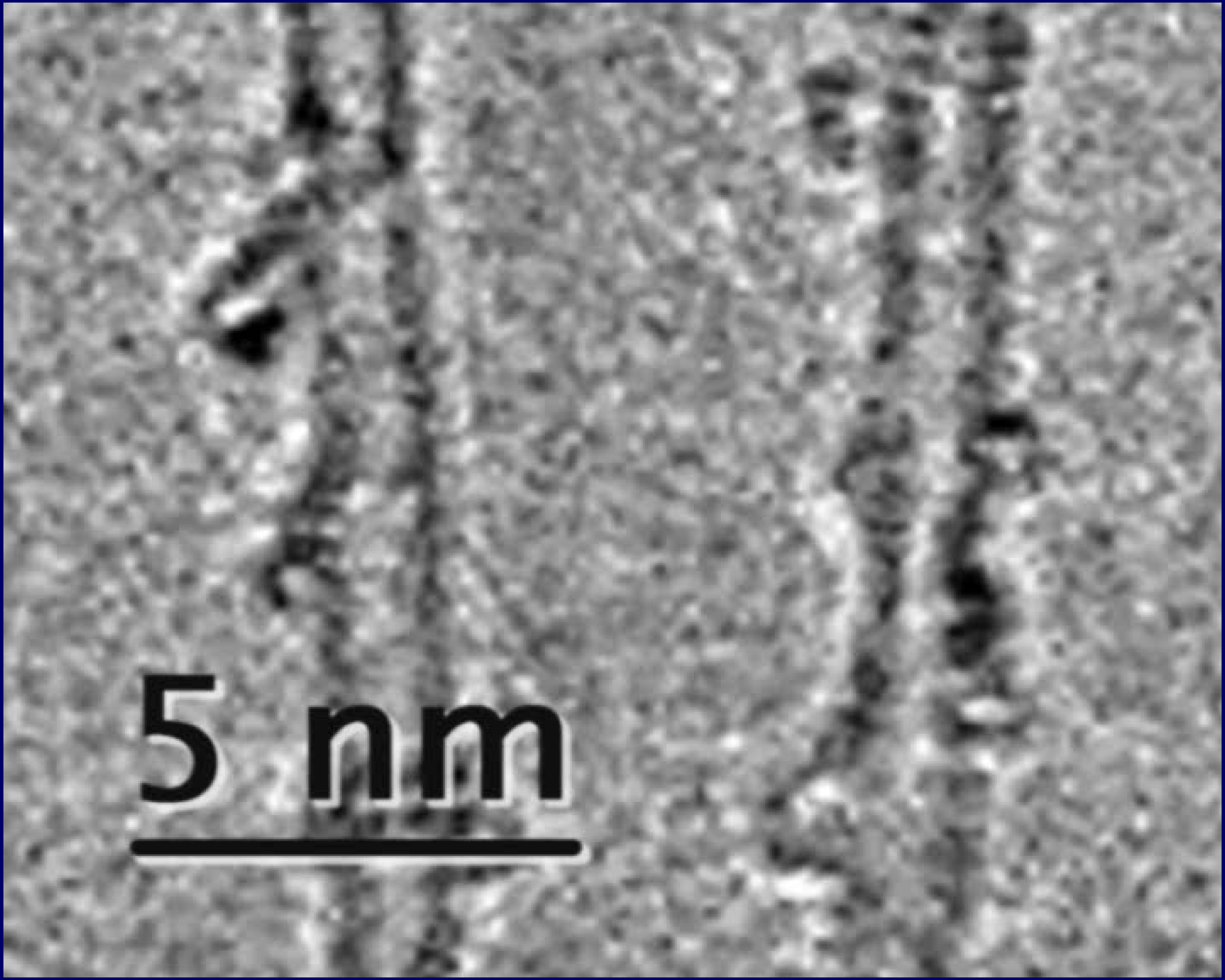

NanoBuds^{TM} on FEI Titan TEM at 80kV with image C_s-corrector - Movie

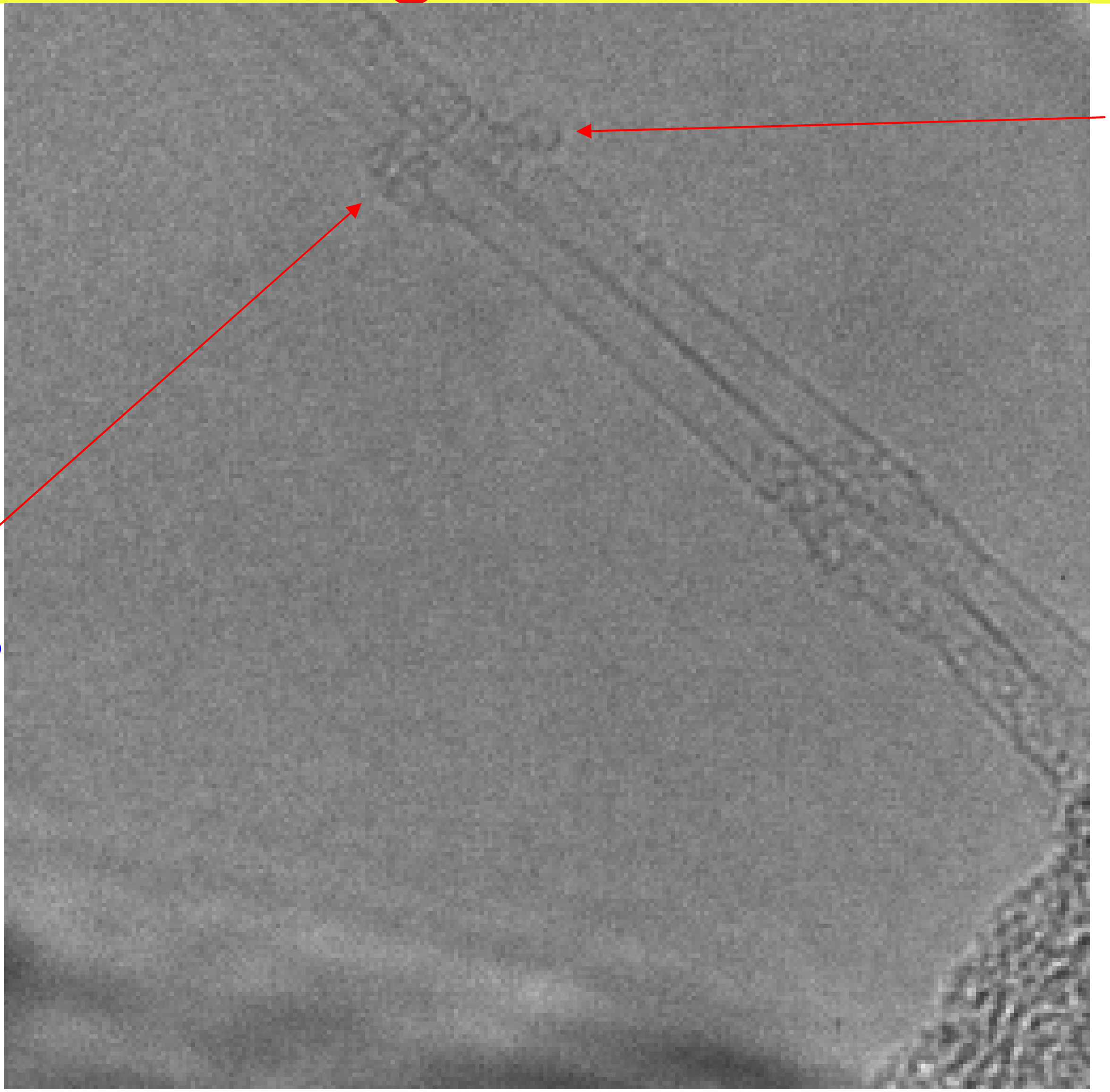

Individual Fullerene

Cluster of Fullerenes

Image :B.Freitag FEI; samples : Prof. Kauppinen HUT

Pulling out CNBs from Hydrofobic Protein Thin Film: Fullerenes remain attached to CNTs

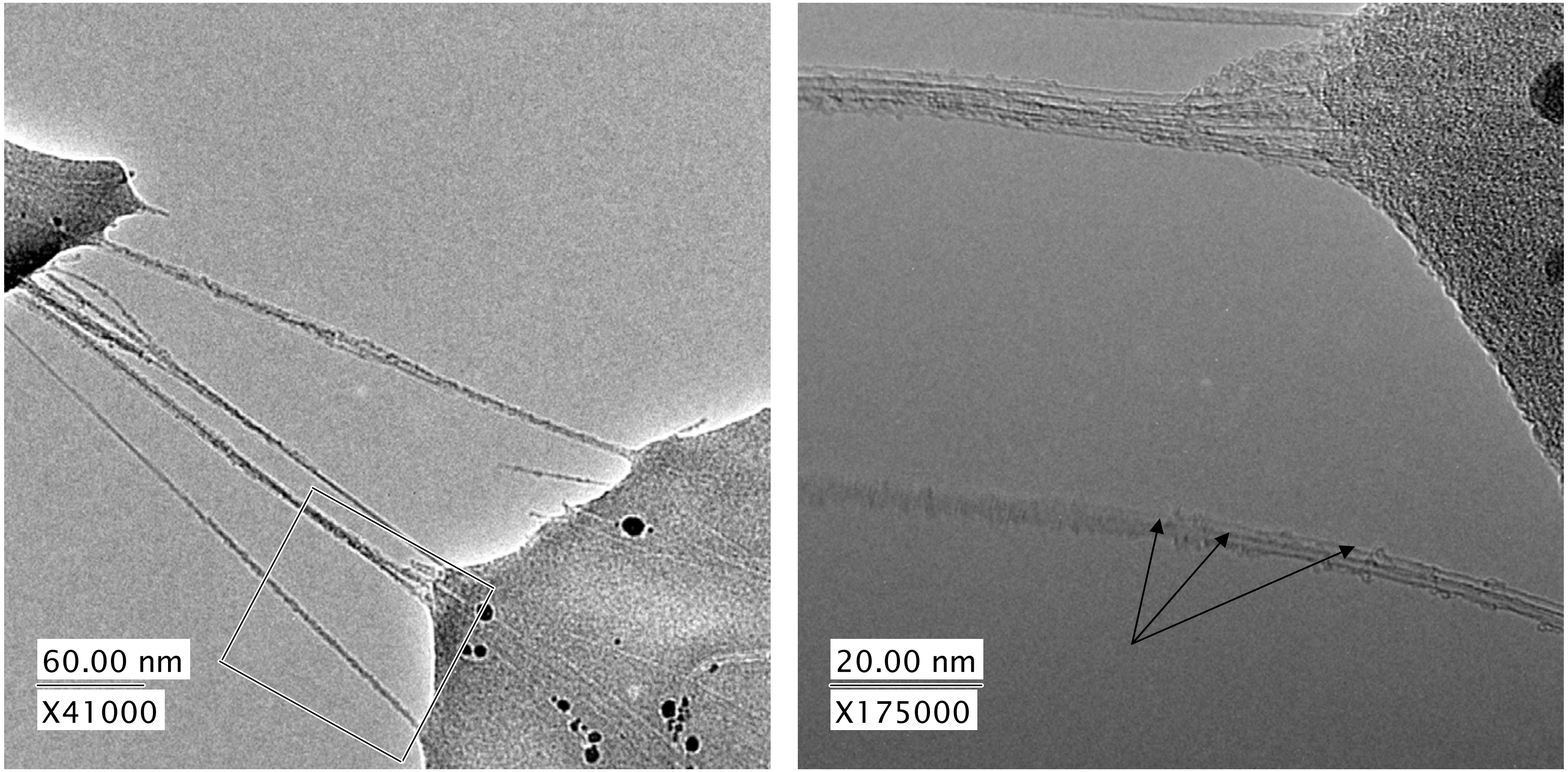

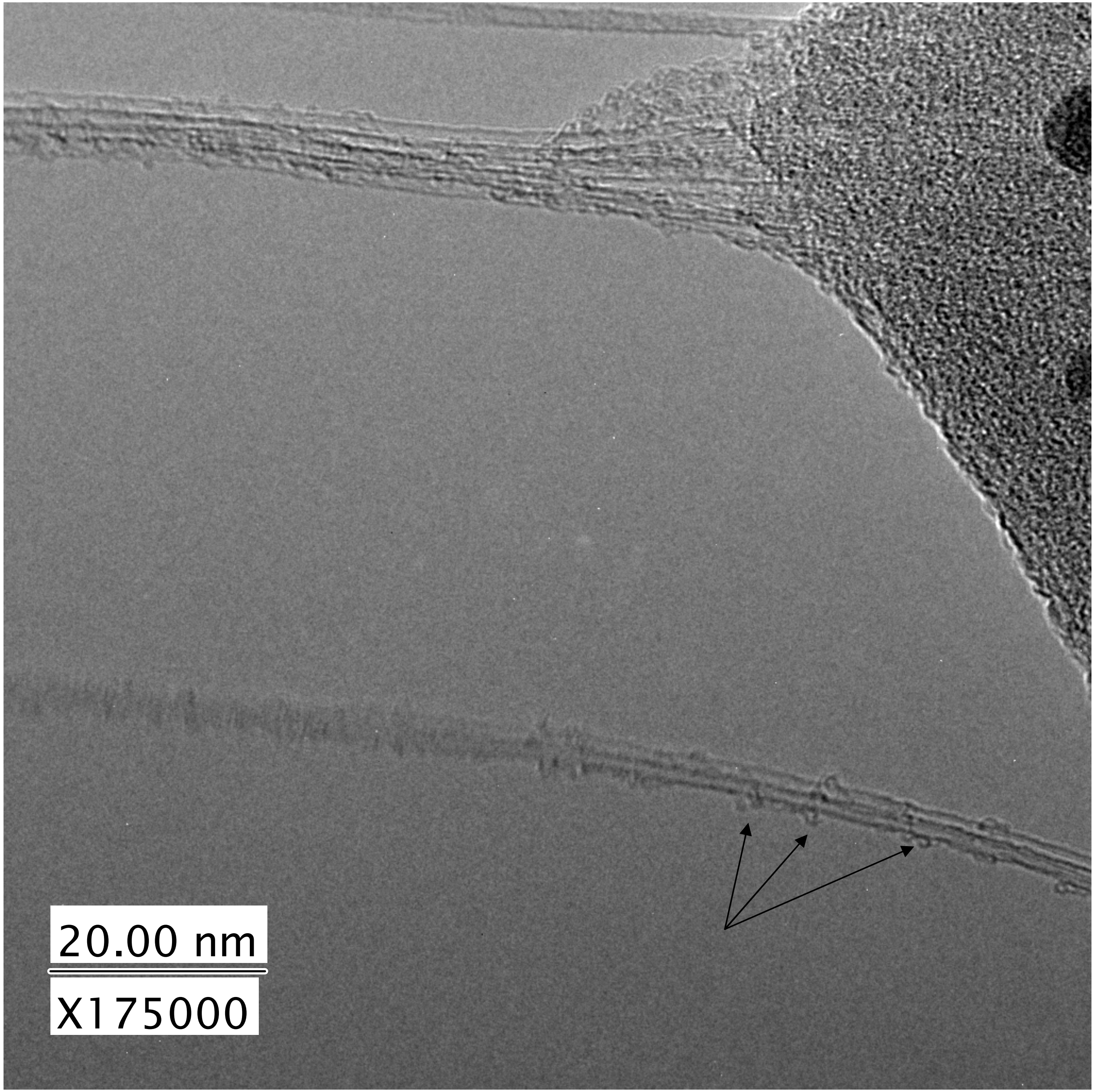
20.00 nm
X175000

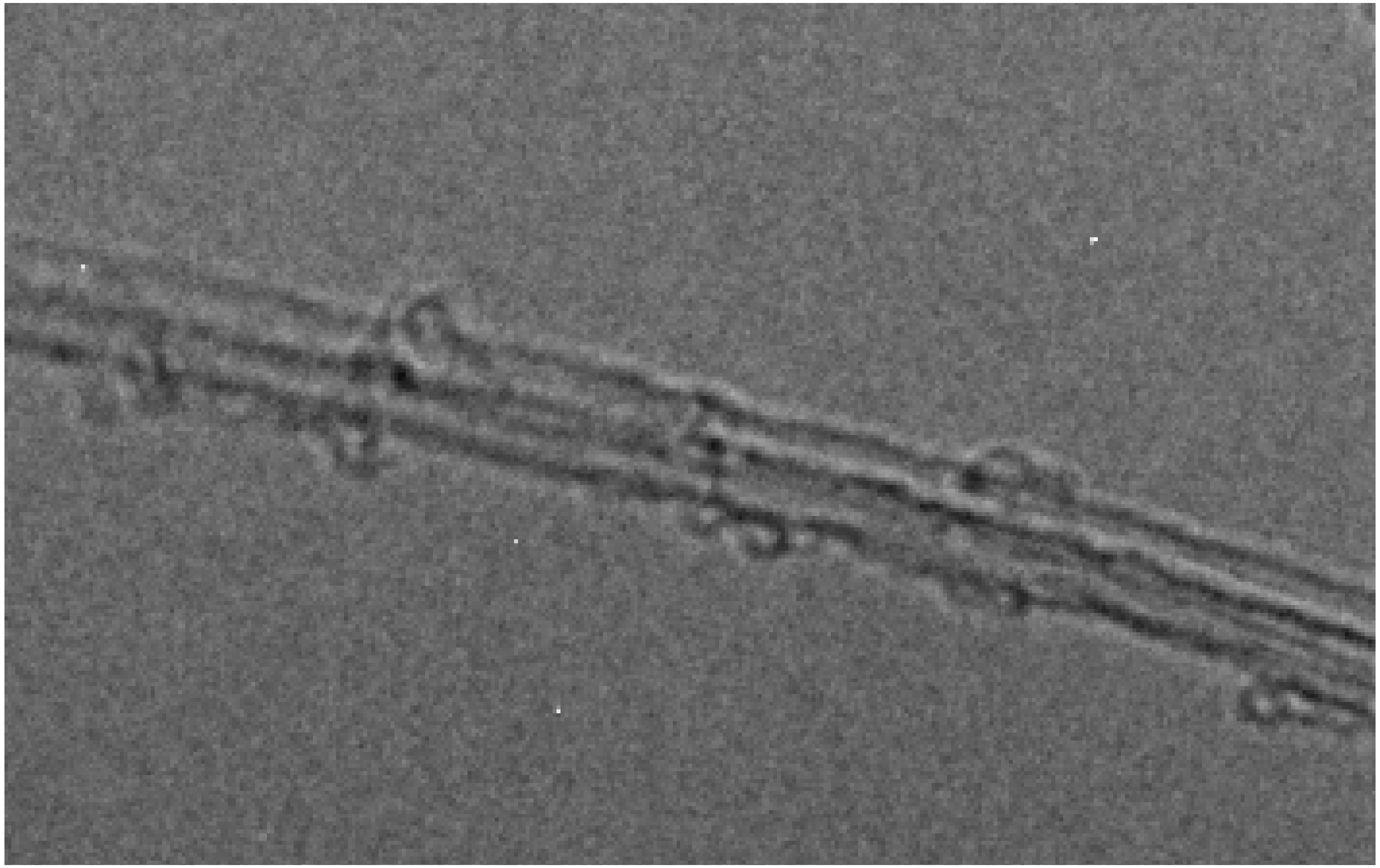

Bonding scenarios of fullerenes on nanotubes based on DFT calculations

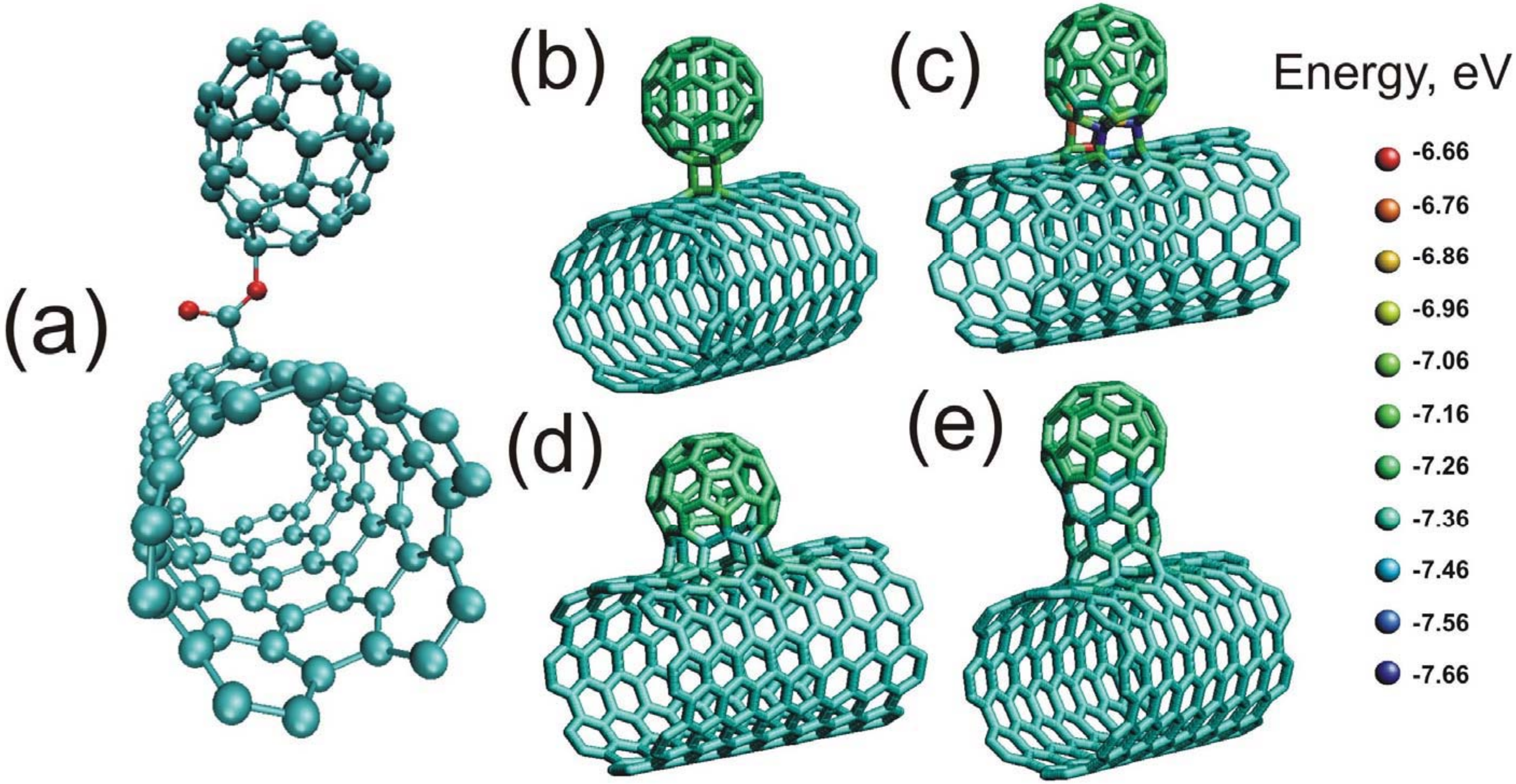

Functionalisation of carbon nanobuds

Electron transport in carbon nanobuds

Transport through nanotube crossings

Transport (percolation) in nanotube networks

Applications:

Low-cost printed electronics: transistors

Gas sensing

Tools:

DFT for geometries and electronic structure

Quantum transport – Green’s function approach

- Conductance of functionalised tubes/buds
- Tunnelling between crossing tubes

Statistical models for percolation transport

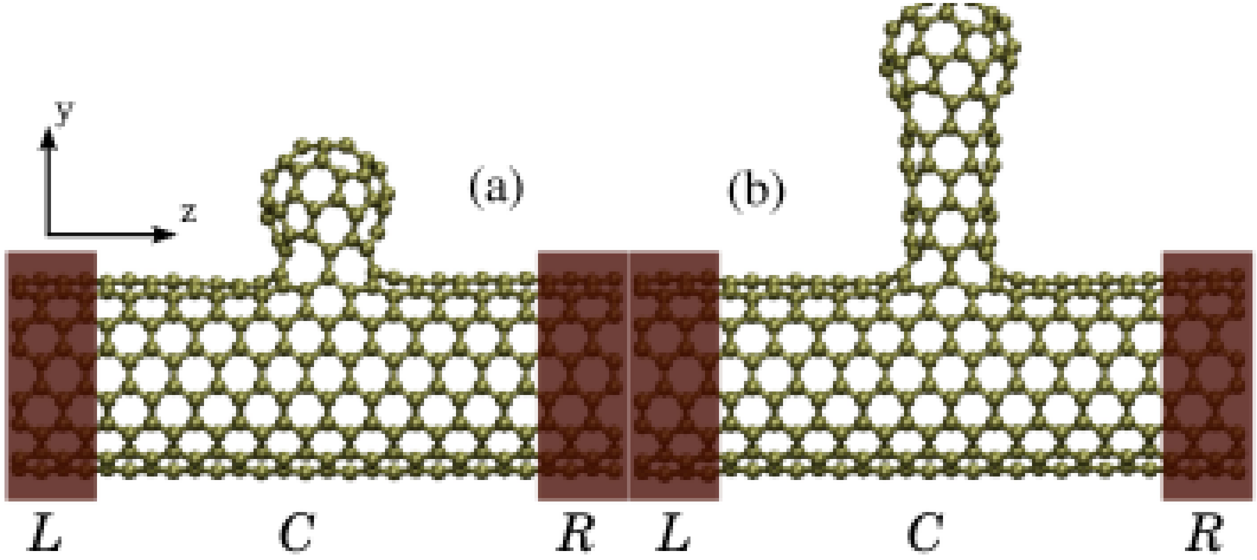

FIG. 1: Typical carbon nanobud (CNB) structures studied in this work. The CNB consists of an imperfect C60 attached to an armchair (8,8) single-wall nanotube (SWNT) via a neck region, made of a (6,0) SWNT. The number of unit cells in the neck region can vary; panel (a) shows a zero-unit-cell neck (CNB0), while (b) shows a two-unit-cell neck (CNB2).

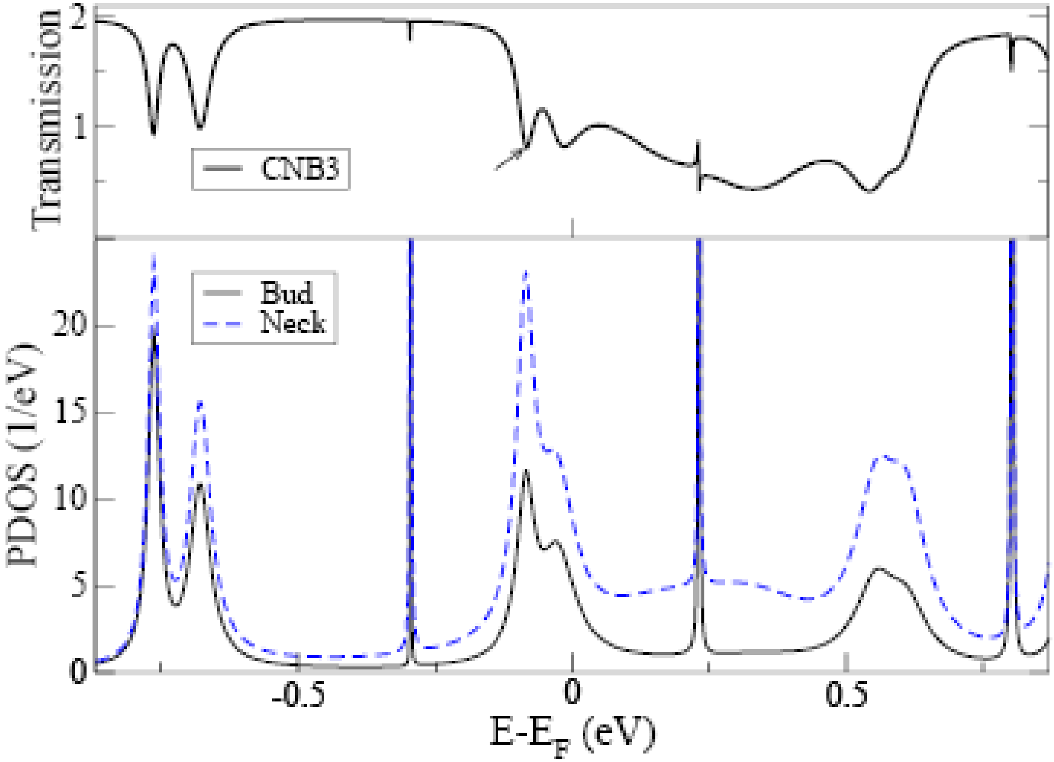

FIG. 3: Projected density of states (PDOS) for the bud and neck part of the CNB3 system (middle panel). There is a strong correlation between PDOS and the transmission shown in the top panel. Bottom: The probability of the eigenchannel scattering states at the dip in transmission indicated by an arrow in the top panel. Comparing left ($T = 0.74$) and right panel ($T = 0.26$) shows that stronger suppression of transmission is related to stronger localization of states in the bud and neck.

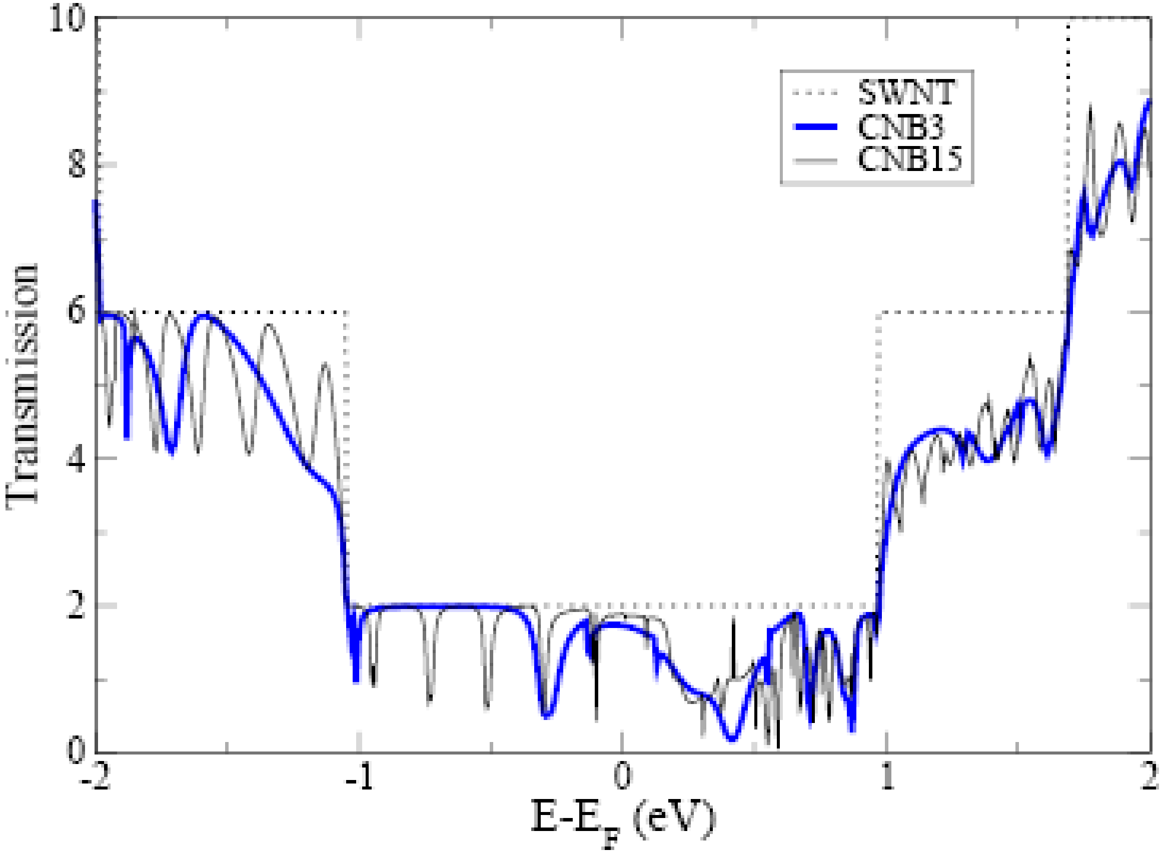

FIG. 4: The transmission for SWNT, CNB3 and CNB15 calculated with a tight-binding model. The trends from first principles are well captured for the smaller CNB3 system. Significantly increasing the system size results in a large number of dips which below E_F display some degree of periodicity.

Conductance sensitive to the bud

Buds can bind gas-phase molecules

Enhanced sensitivity to sensing

Introduction: Nanotube Cross Junctions

(Paula Havu, Javad Hashemi)

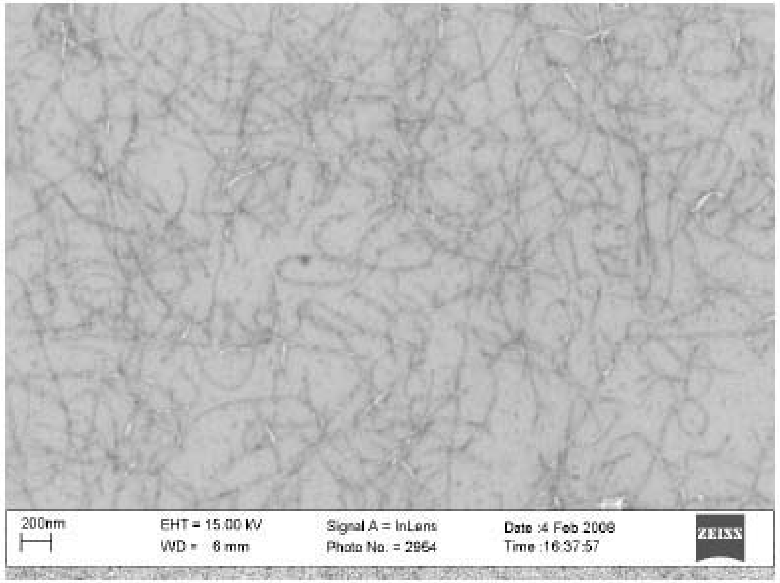

Nanotube bundle network.

Figure: Nano Materials Group,
Aalto University

- Experiments:
  - Metal-metal (MM) junctions and semiconductor-semiconductor (SS) junctions 100-2300 kΩ.
  - Semiconductor-metal (SM) 32 MΩ.

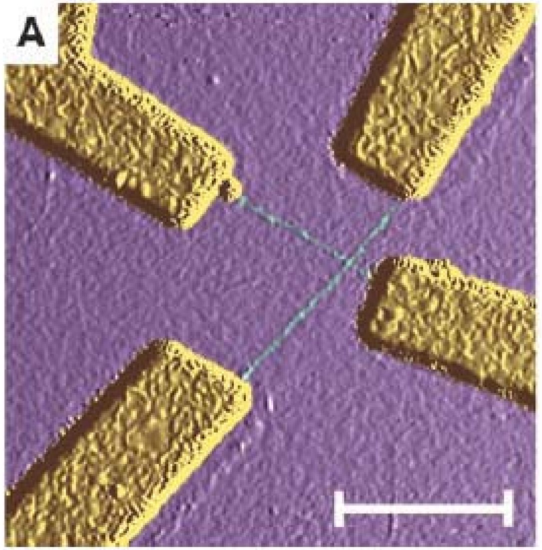

- M.S.Fuhrer *et al.* Science **288**, 494 (2000).
- B.Gao, *et al.* Phys. Rev. Lett. **92**, 216804 (2004).
- P. N. Nirmalraj et al. NanoLett. 9, 3890 (2009).

Model

- 2 nanotubes:
  - (8,8)-metallic
  - (14,0)-semiconducting

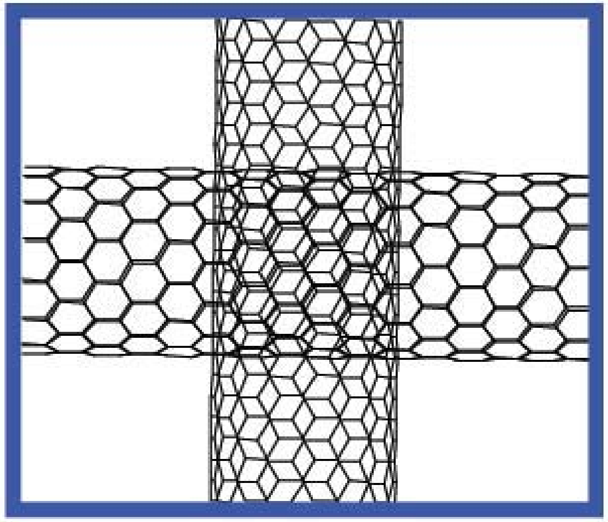

- Up to 896 atoms

- Electronic structure from the density functional theory calculations
  - All electron code FHI-aims [1] with PBE xc-functional
  - Van der Waals correction [2]
  - Transport calculations from Landauer-Büttiker formula

$$G = \frac{2e^2}{\pi} \int_{-\infty}^{\infty} T(E) \left(-\frac{\partial f(E)}{\partial E} \right) dE$$

1) V. Blum, R. Gehrke, F. Hanke, P. Havu, V. Havu, X. Ren, K. Reuter and M. Scheffler, Comp. Phys. Comm. 180, 2175-2196 (2009).

2) Tkatchenko et al. PRL 102 073005 (2009)

Transport properties of junctions

Junction:

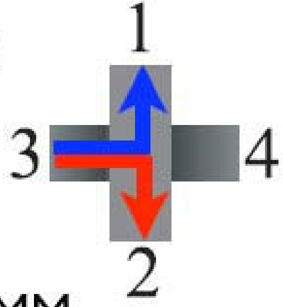

$$G = \frac{2e^2}{\pi}\int_{-\infty}^{\infty} T(E)\left(-\frac{\partial f(E)}{\partial E}\right) dE$$

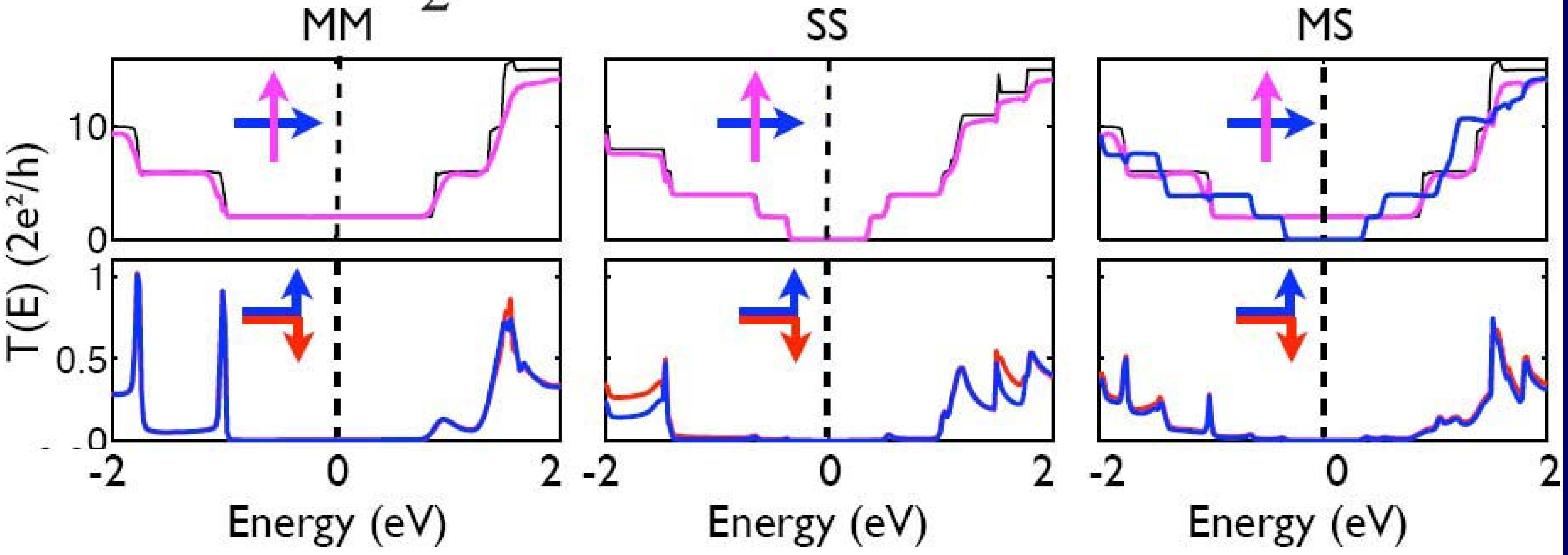

Effect of charge doping / gate

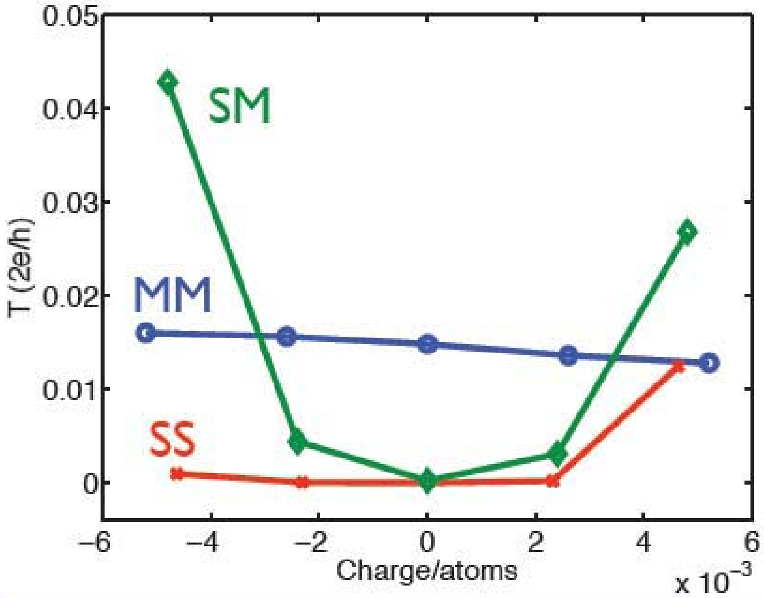

- MM: conductance almost constant
- SS: conductance small and asymmetric
- SM: depletion region

MM pos.

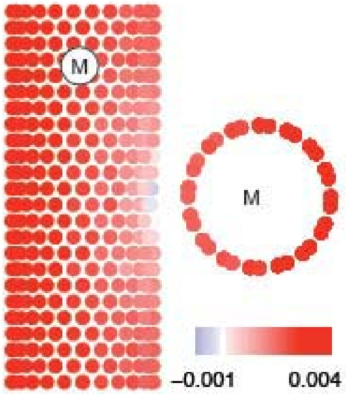

SS neg.

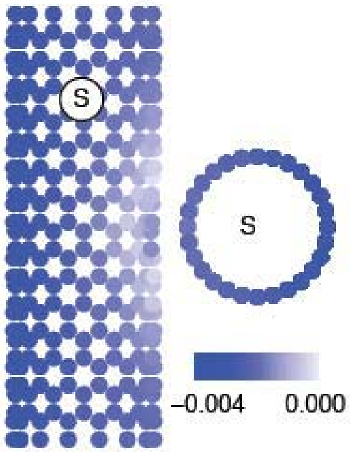

SM neg.

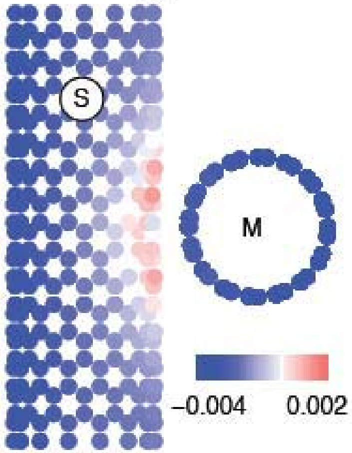

SM pos.

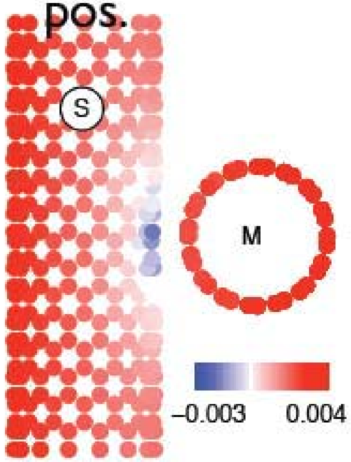

As a function of distance

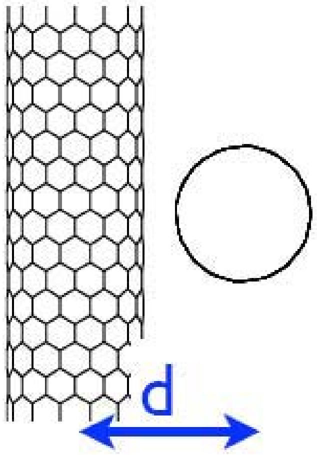

- At shorter nanotube distances more atoms are at the junction region

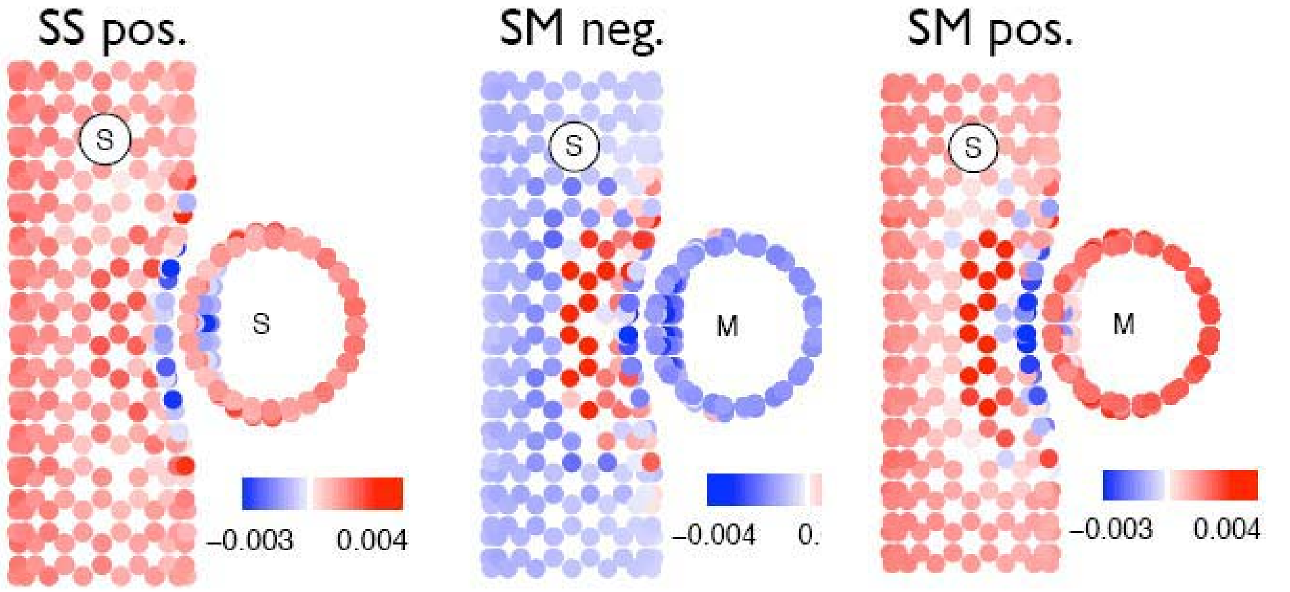

As a function of distance

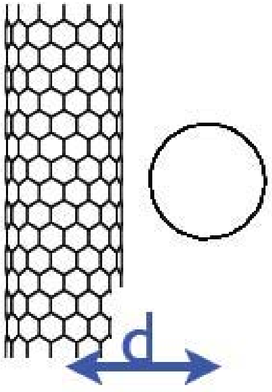

- MM: first conductance increases and then degreases.
- SS: similar oscillations in conductance, but smaller amplitude
- SM: conductance increases

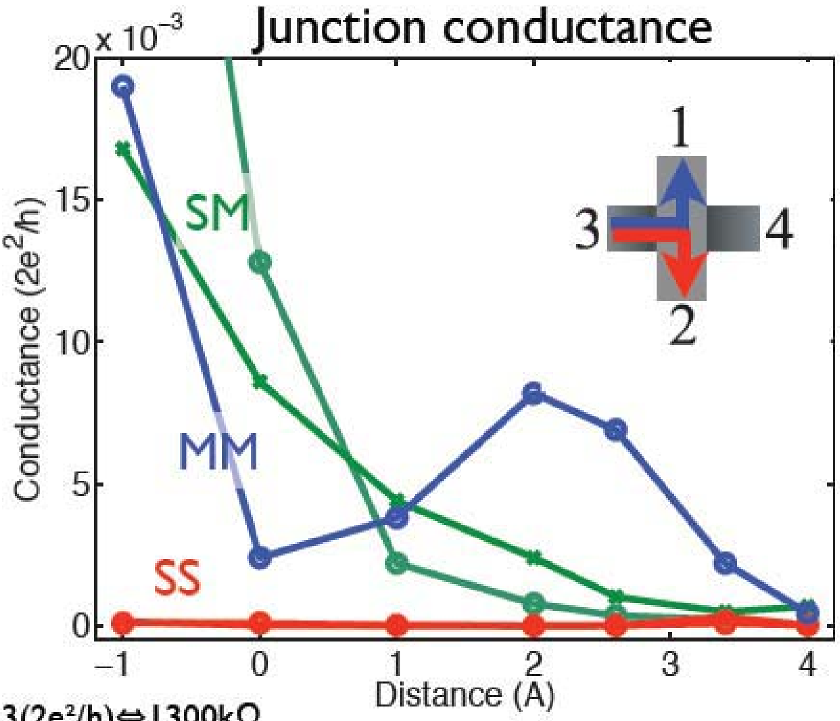
Junction conductance

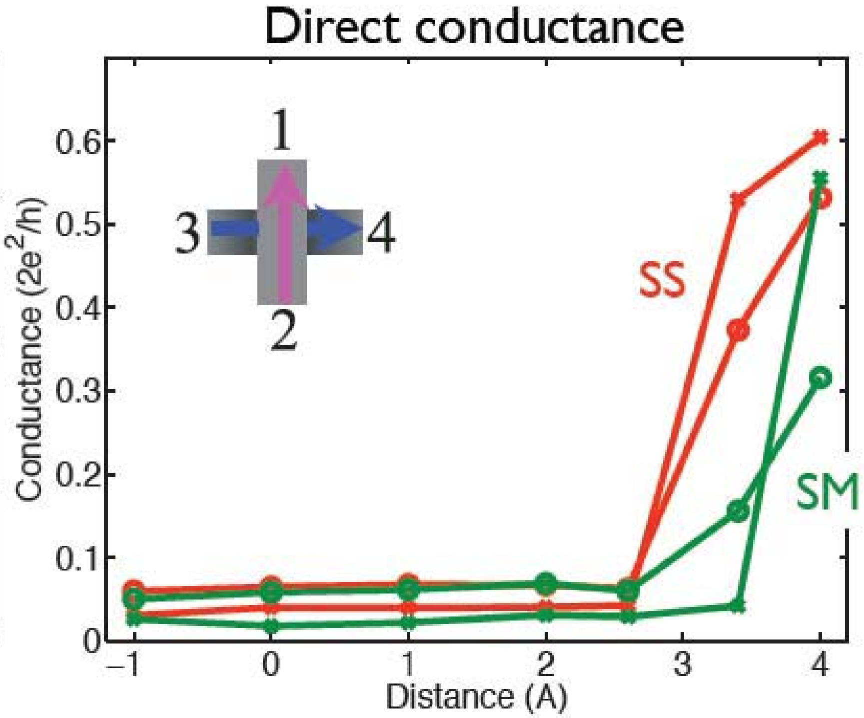
Direct conductance

10e-3($2e^2/h$)⇔1300kΩ

2. Transition metal atoms on a defected graphene sheet

(Arkady Krasheninnikov)

Motivations:

- Possible Kondo effect in graphene: the knowledge of the realistic electronic structure is required
- Tuning of the local electronic and magnetic structure of graphene
- Recent TEM experiments on migration of individual metal atoms chemisorbed on graphene

$T_K \sim \exp(-1/NJ)$

K. Sengupta and G. Baskaran, PRB 77 (2008) 045417

Y. Gan, L. Sun, F. Banhart, Small (2008)

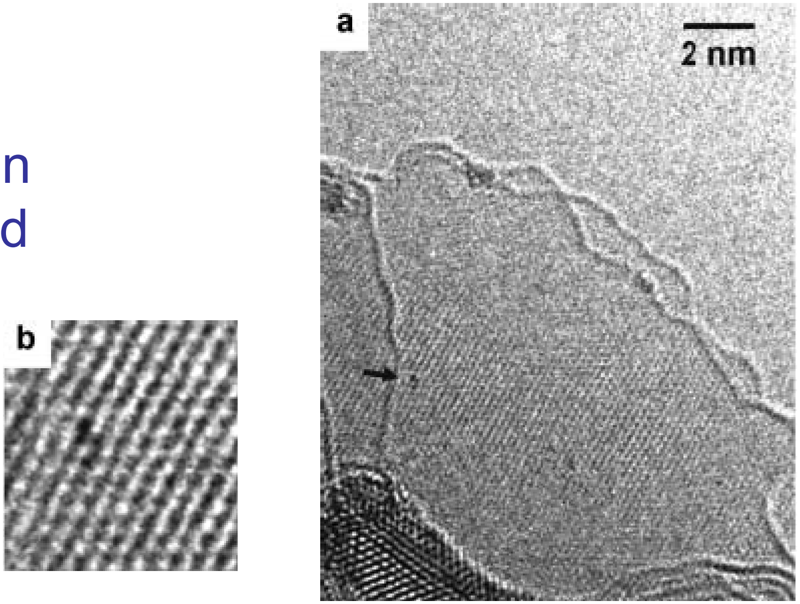

Transition metal atoms on a defected graphene sheet

Further motivations :

- Similar to Pt, Pd, Ni, and other metal nanoparticles on carbon nanotubes, very interesting catalytic properties should be expected
- Understanding the interaction of transition metal atoms with *sp*^{2}-bonded carbon is important for a better control over growth of carbon nanotubes and graphene

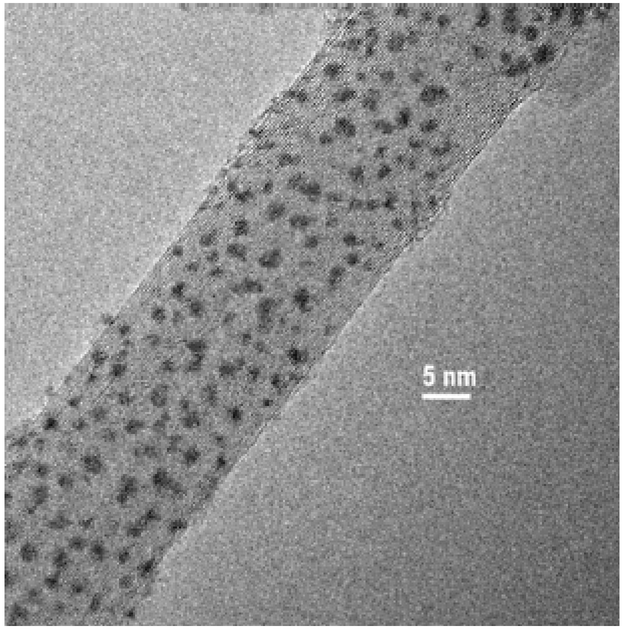

C. Bittencourt *et al.*, Chem. Phys. Lett. **462** (2008) 260

TM atoms on graphene: the simulations

Spin-polarized DFT with GGA/PAW, plane waves (VASP)

Krasheninnikov *et al*, PRL **102 (2009) 126807**

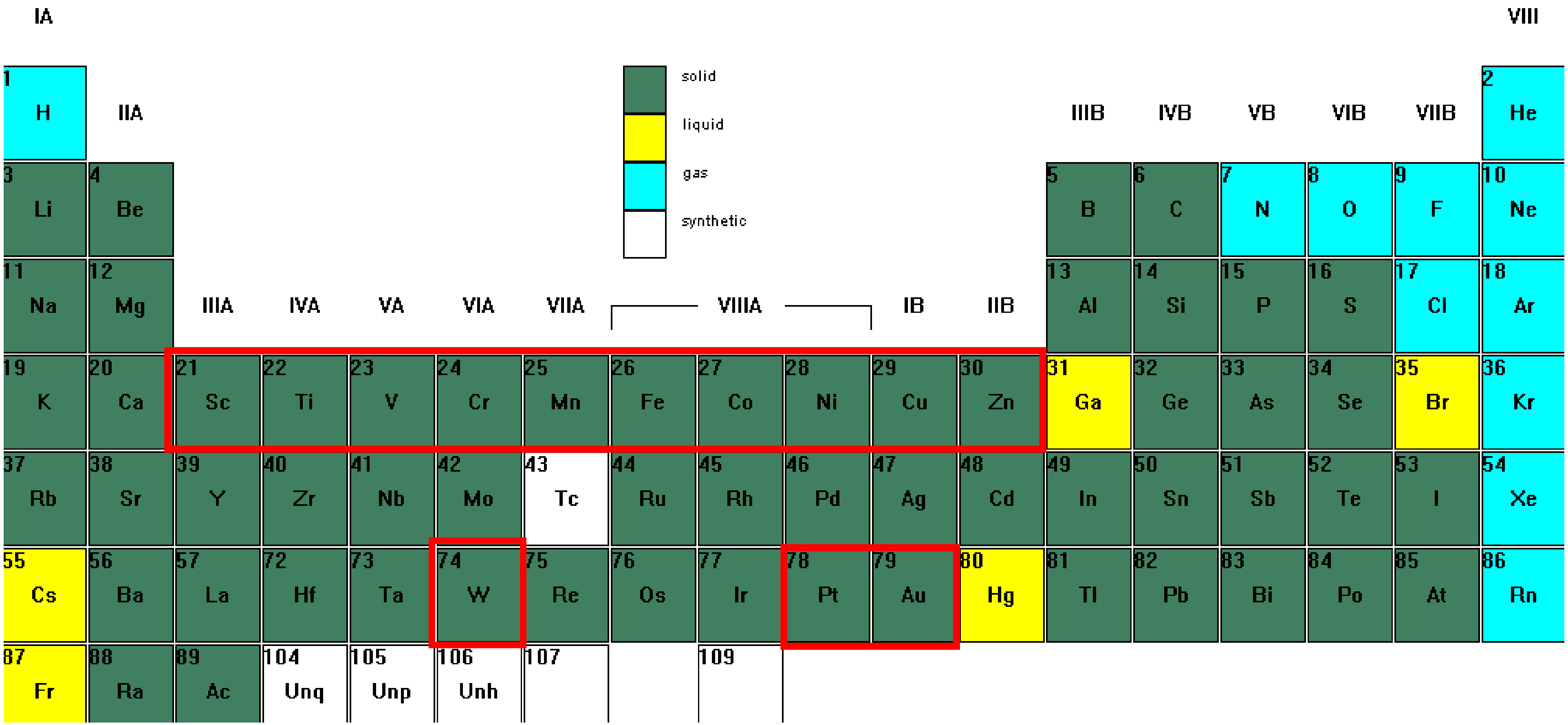

🟩 solid
🟨 liquid
🟦 gas
⬜ synthetic

IA																	VIII
1 H	IIA											IIIB	IVB	VB	VIB	VIIB	2 He
3 Li	4 Be											5 B	6 C	7 N	8 O	9 F	10 Ne
11 Na	12 Mg	IIIA	IVA	VA	VIA	VIIA		VIIIA		IB	IIB	13 Al	14 Si	15 P	16 S	17 Cl	18 Ar
19 K	20 Ca	21 Sc	22 Ti	23 V	24 Cr	25 Mn	26 Fe	27 Co	28 Ni	29 Cu	30 Zn	31 Ga	32 Ge	33 As	34 Se	35 Br	36 Kr
37 Rb	38 Sr	39 Y	40 Zr	41 Nb	42 Mo	43 Tc	44 Ru	45 Rh	46 Pd	47 Ag	48 Cd	49 In	50 Sn	51 Sb	52 Te	53 I	54 Xe
55 Cs	56 Ba	57 La	72 Hf	73 Ta	74 W	75 Re	76 Os	77 Ir	78 Pt	79 Au	80 Hg	81 Tl	82 Pb	83 Bi	84 Po	85 At	86 Rn
87 Fr	88 Ra	89 Ac	104 Unq	105 Unp	106 Unh	107		109									

Transition metal adatoms on a pristine graphene sheet

Fe, Co, Ni

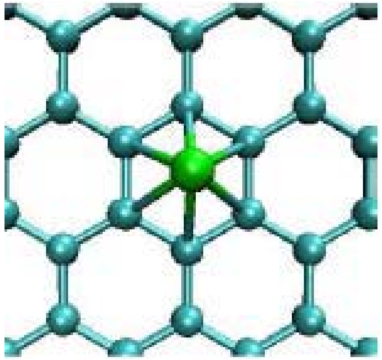

Pt

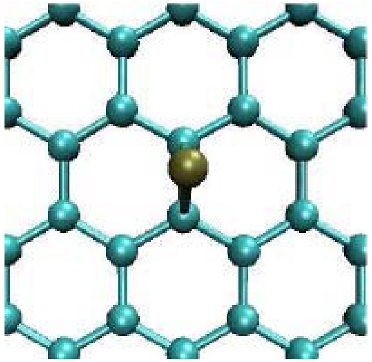

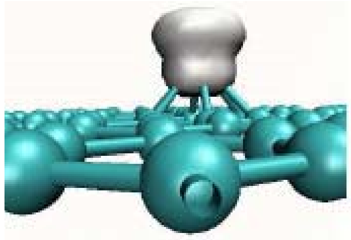

Fe, spin density

	Au	Pt	Fe	Co	Ni
E_{ad} (eV)	-0.13	-1.51	-1.03	-1.50	-1.46
M (μ_B)	0.99	0.00	1.99	1.14	0.00

- Migration barriers 0.2-0.8 eV :
- Mobile at room temperature;
  Difficult to achieve control over the precise position of adatoms;

The results are in agreement with several recent works:

- ☐ Sevincli *et al*., PRB 77, 195434 (2008),
- ☐ K. T. Chan *et al*., PRB 77, 235430 (2008),
- ☐ Suarez-Martinez *et al*., to be published.

Metal atoms at single vacancies in graphene sheets: the structure

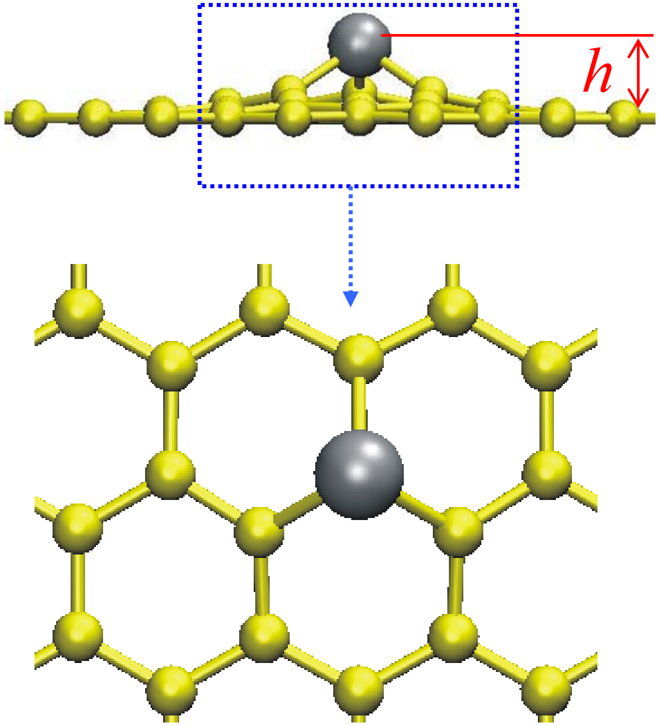

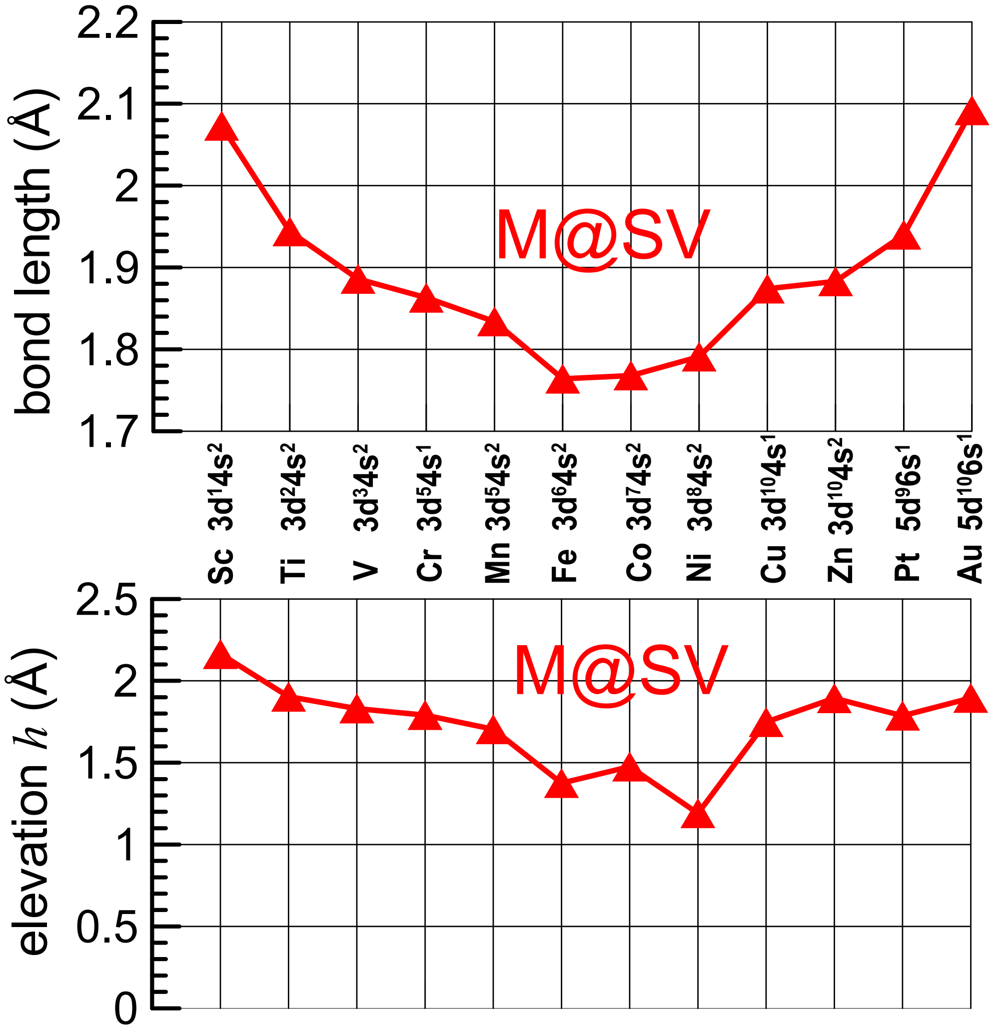

The structure is not flat;
TM atoms are "too big" to fit in

Metal atoms at single vacancies in graphene sheets: the bonding

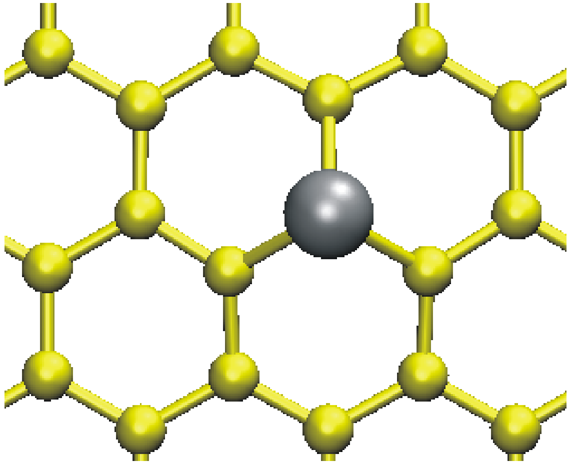

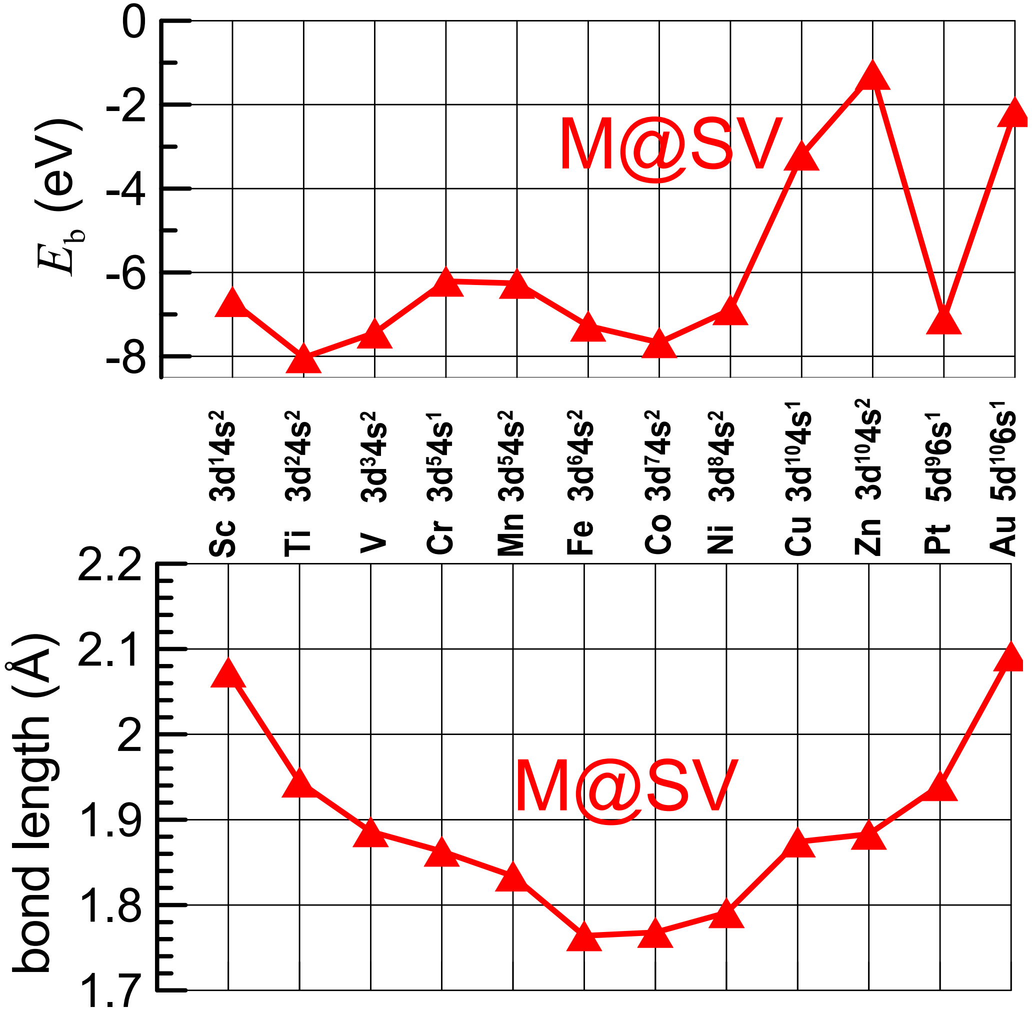

- Bonding is strong!
- Binding energy (<0) is the lowest for metals which form carbides
- Ti ($3d^24s^2$, 4 valence el.) has the lowest energy

TM atoms at double vacancies

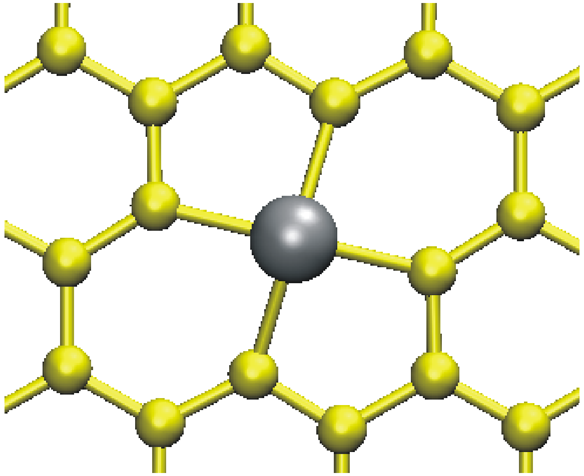

One exception: V

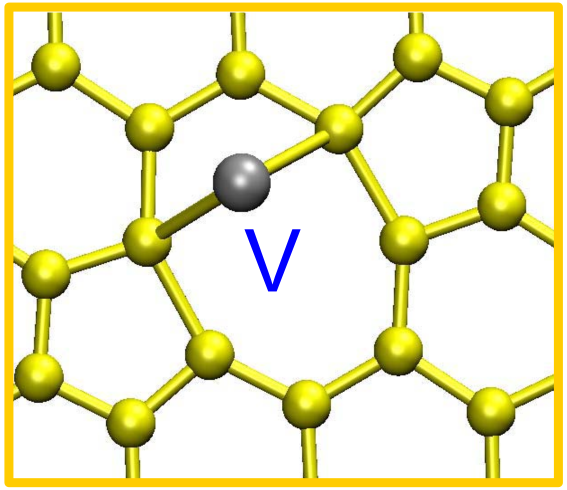

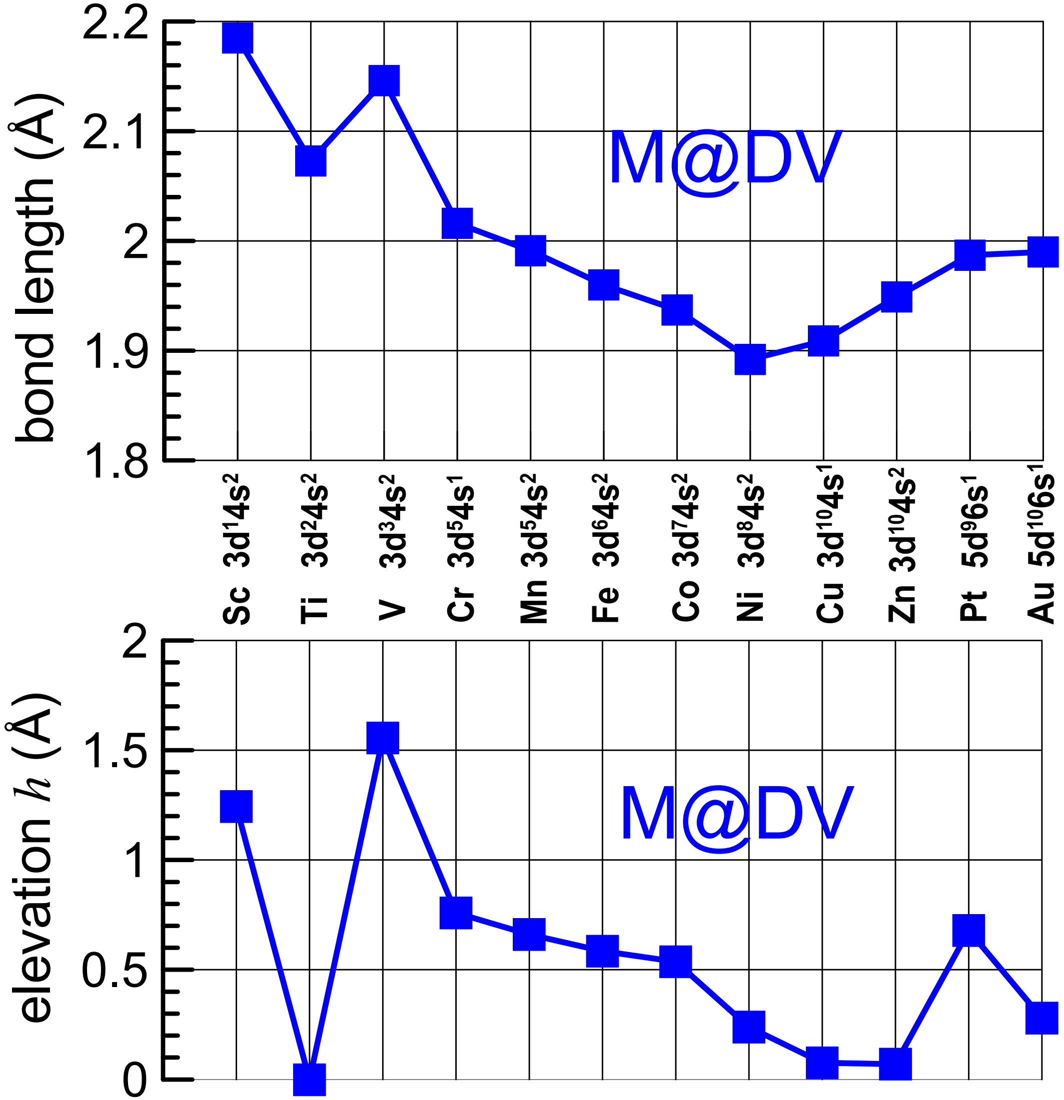

TM atoms at double vacancies

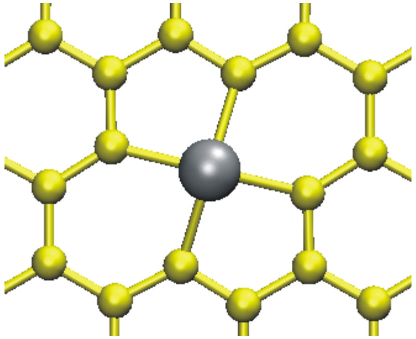

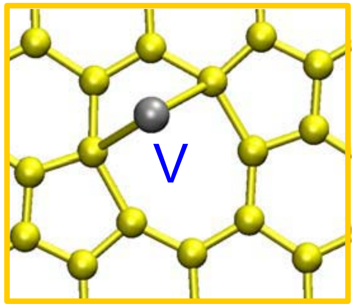

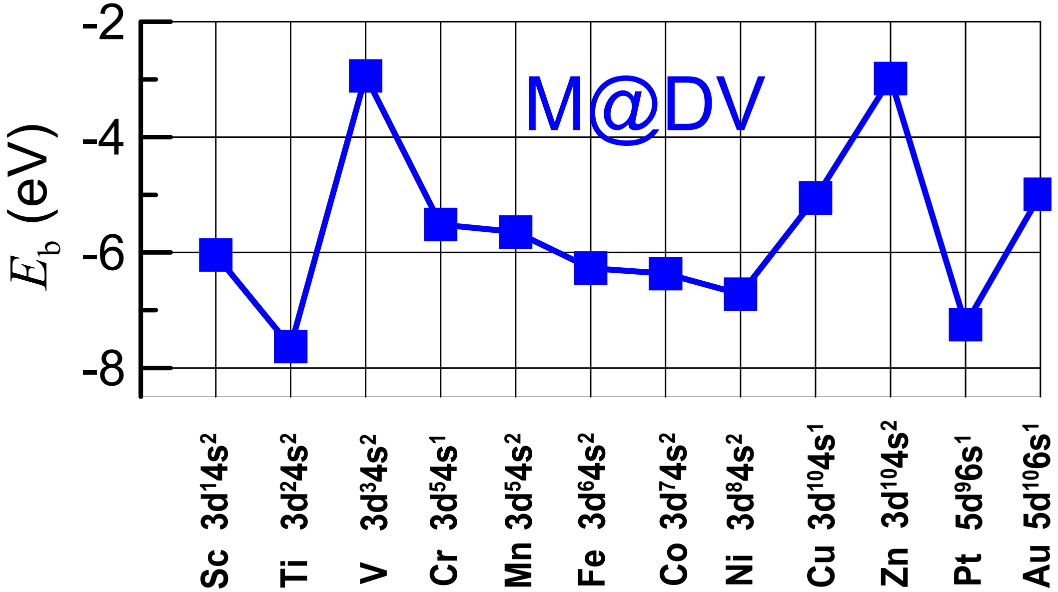

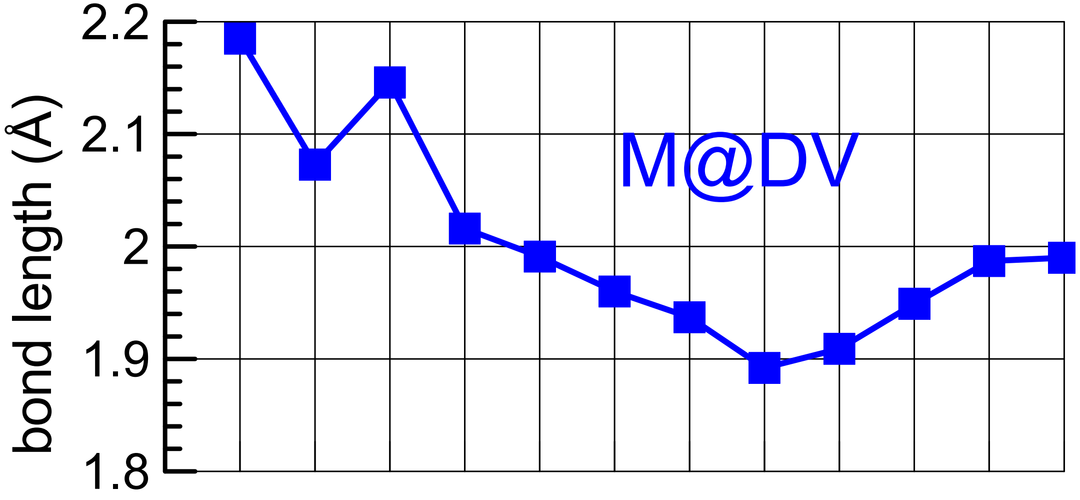

- Bonding is strong, as in the case of single vacancies!
- V binds weakly due to two bonds only
- Ti and Au complexes are almost flat

TM@vacancies: binding and magnetism

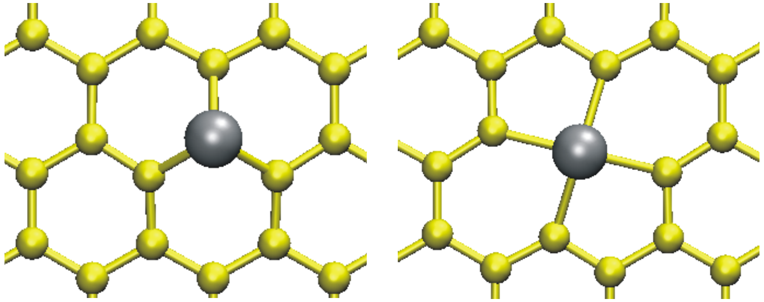

Qualitative picture

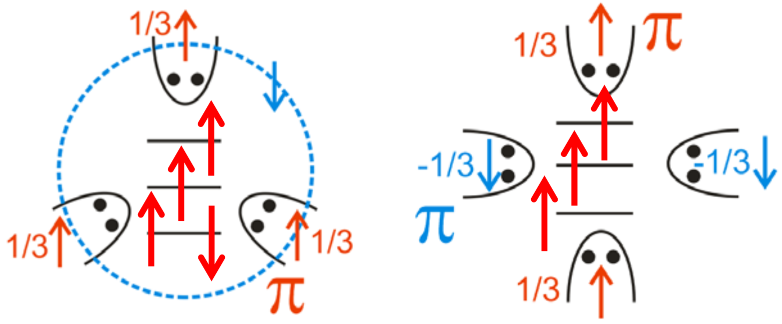

Ti: 4 e, M=0
V: 5 e, M=1
Cr: 6 e, M=2
Mn: 7 e, M=3
Fe: 8 e, M=0: e-e repulsion

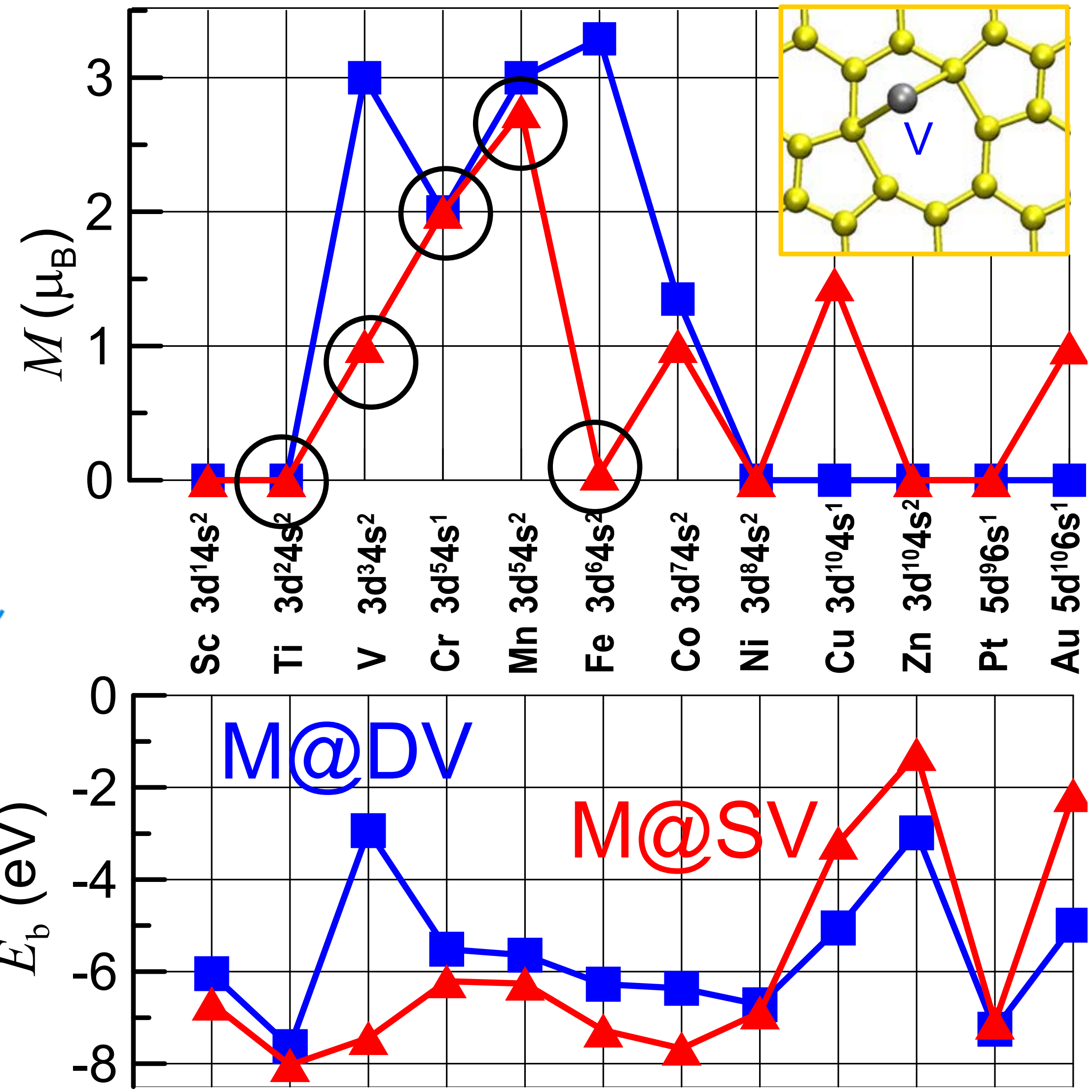

Magnetism: the quantitative picture

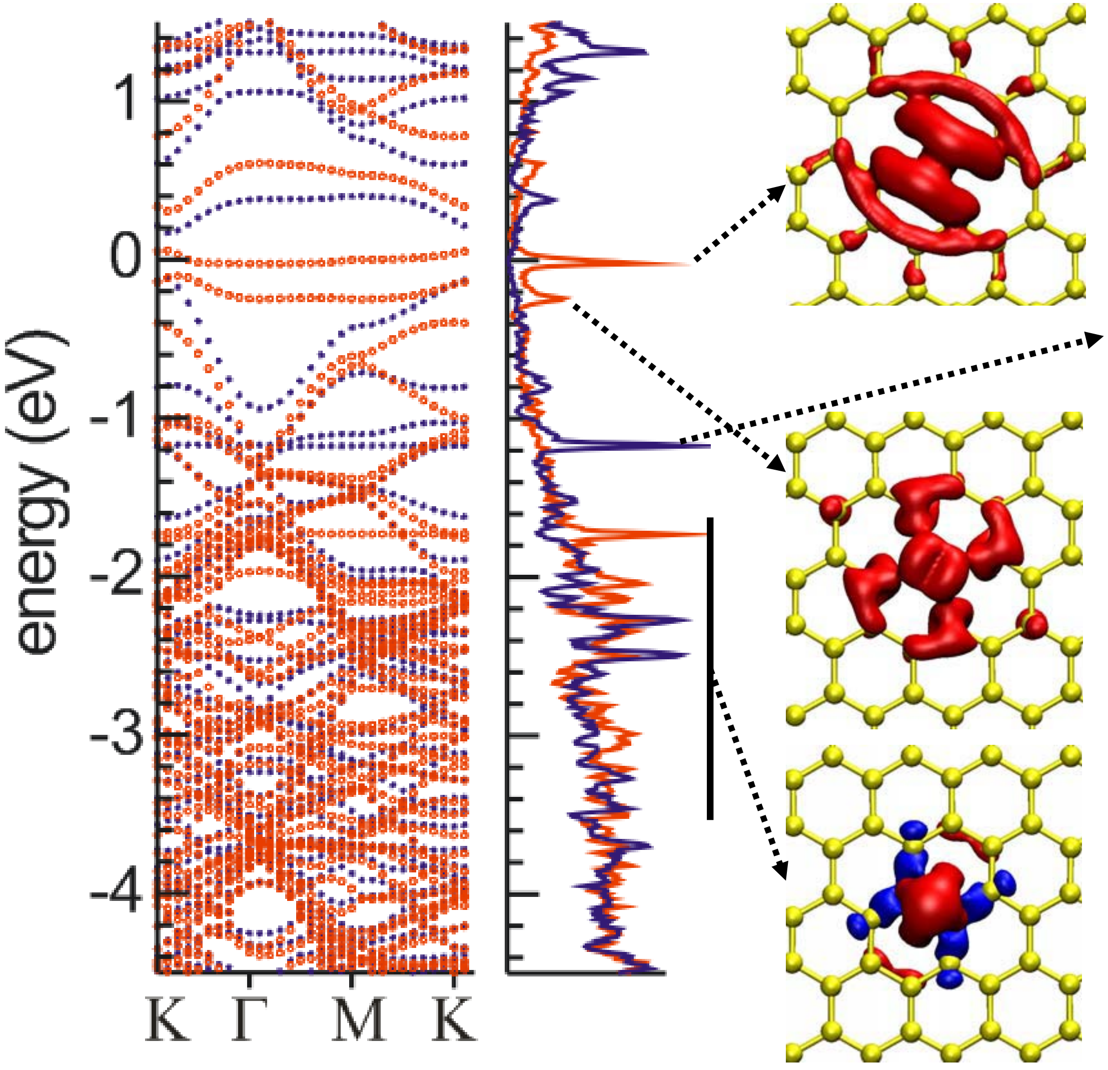

Mn@DV

Energy-resolved magnetization density

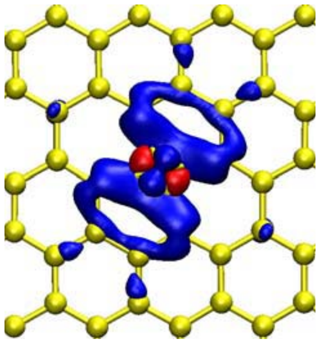

Total magnetization density

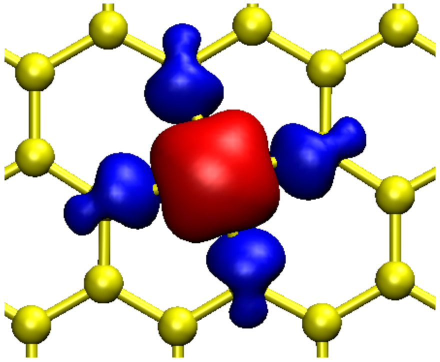

Both *d*-states of transition metal atoms and *σ*/*π*-states of neighboring C atoms contribute to the magnetization;

For Au and Cu, a considerable part of the magnetization comes from *s* and *p* states;

Mobility of atom@SV/DV complexes

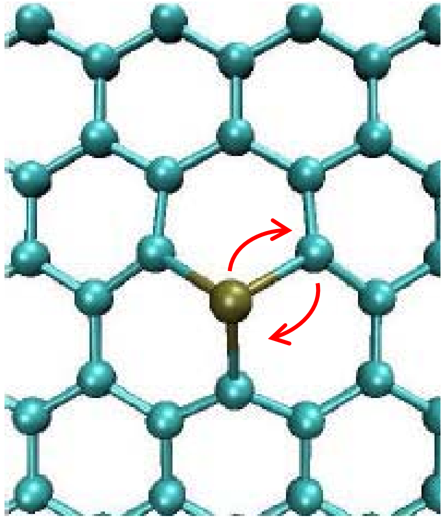

- Nudged elastic band method, DFT GGA/PAW

	Au	Pt	Fe	Co	Ni
@SV	2.1	3.1	3.6	3.2	3.1
experim.	2.4*	2.6*			
@DV	5.1	6.0	5.3	6.3	6.2

*** Y. Gan, L. Sun, F. Banhart, Small (2008)**

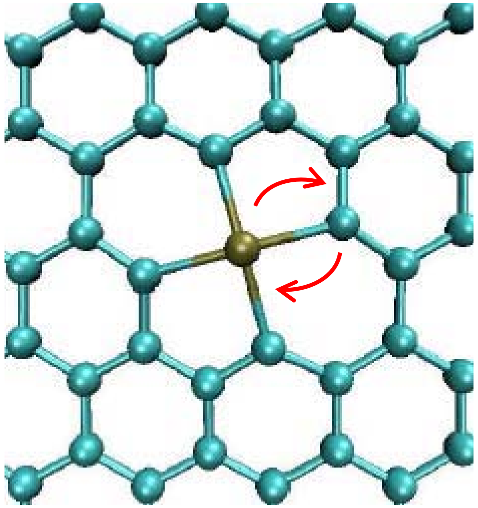

Naked SV ~ 1.4 eV
Naked DV ~ 7 eV

- TM@SV complexes are be immobile at room and even moderate (100-200C) elevated temperatures

- TM@DV are immobile even at high temperatures

Possible experimental realization

- electron beam in modern TEMs can be focused onto a sub-Å^2 area
- Knock-out of individual atoms is possible

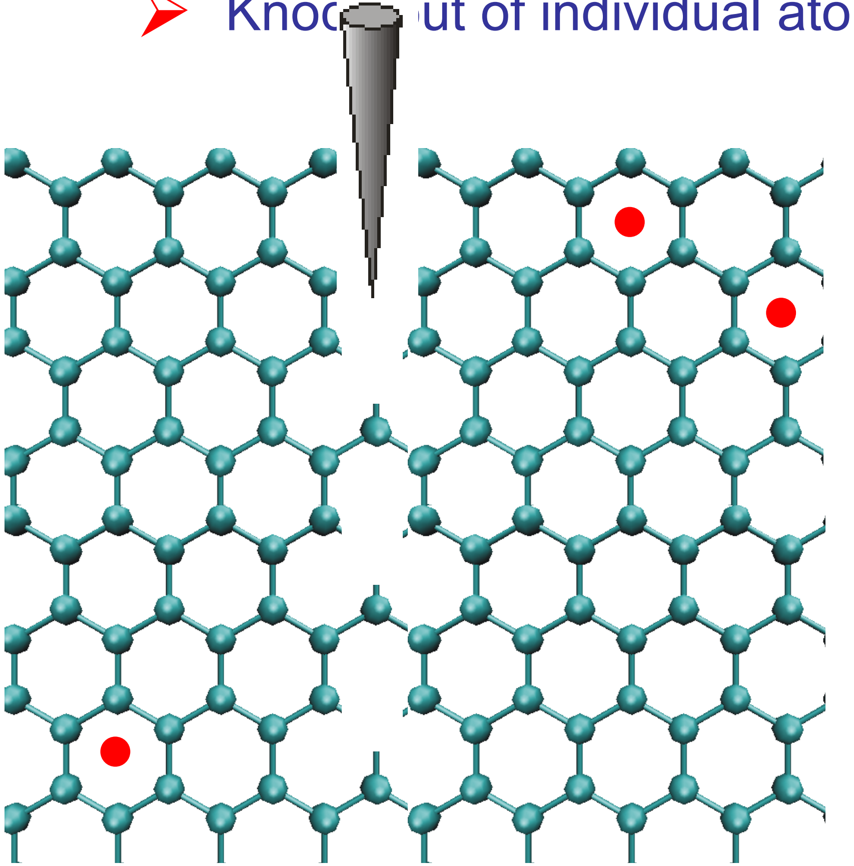

- Graphene flakes with adsorbed metal atoms can be synthesized as in

  Y. Gan, L. Sun, F. Banhart, Small (2008)

- Increasing the temperature (plus e-beam sputtering of metal particles) will make the metal atoms mobile
- Vacancies should pin the metal atoms
- Focused ion beams can also be used

3 (a) Ferroelectric perovskites

(Riku Oja, poster)

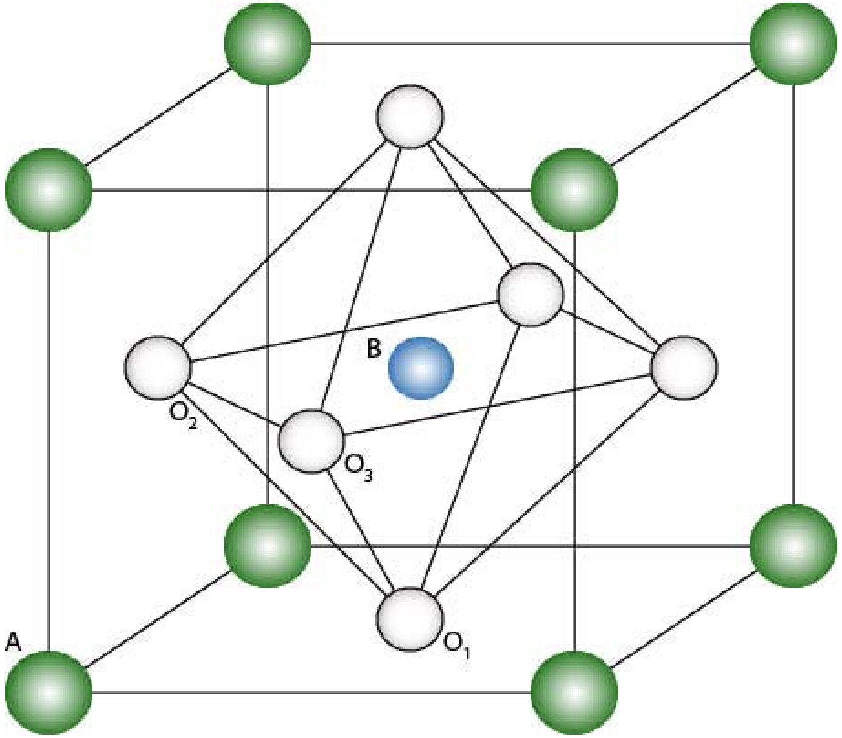

General ABO_3 *perovskite in the cubic (non-polarized) phase*

- Perovskites exhibit interesting dielectric and electromechanical phenomena
- Applications in memories and sensors
- Very sensitive to small deformations, high accuracy required in DFT

Perovskite superlattices

- *Charge-imbalanced interfaces* may lead to 2D metallicity [1]
- Anomalous volume and permittivity [2] caused by interfacial ionic displacements [3]

[1] A. Ohtomo et al., Nature **419** 378 (2002)
[2] J. Narkilahti et al., Phys. Rev. B **79** 014106 (2009)
[3] R. Oja and R. M. Nieminen, Phys. Rev. B **80** 205420 (2009)

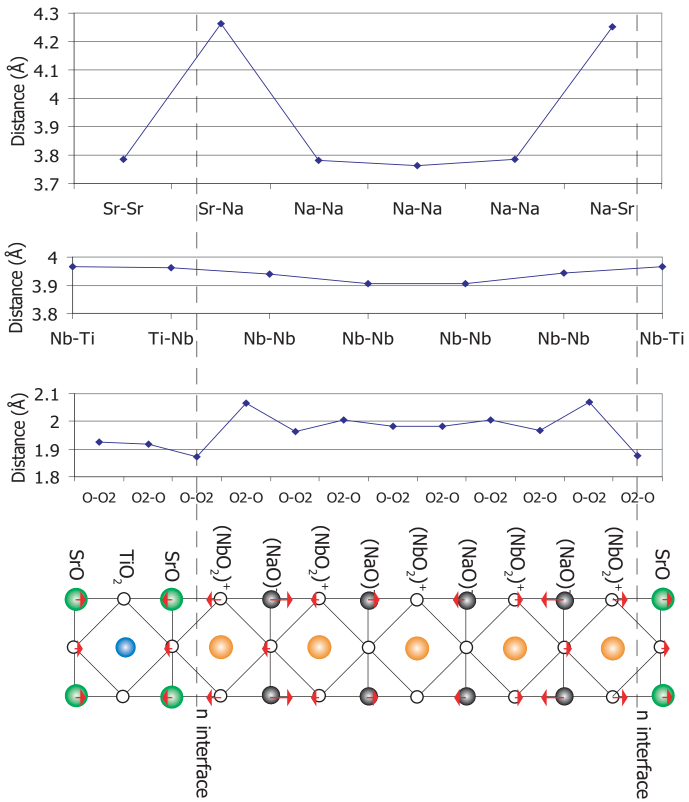

Lattice expansion: ionic distances in $NaNbO_3/SrTiO_3$ superlattice with two n interfaces

Strain-induced ferroelectricity

- *Incipient ferroelectrics* may become ferroelectric when *epitaxially strained*
- In cooperation with University of Oulu, first verification of strain-induced ferroelectricity [4]

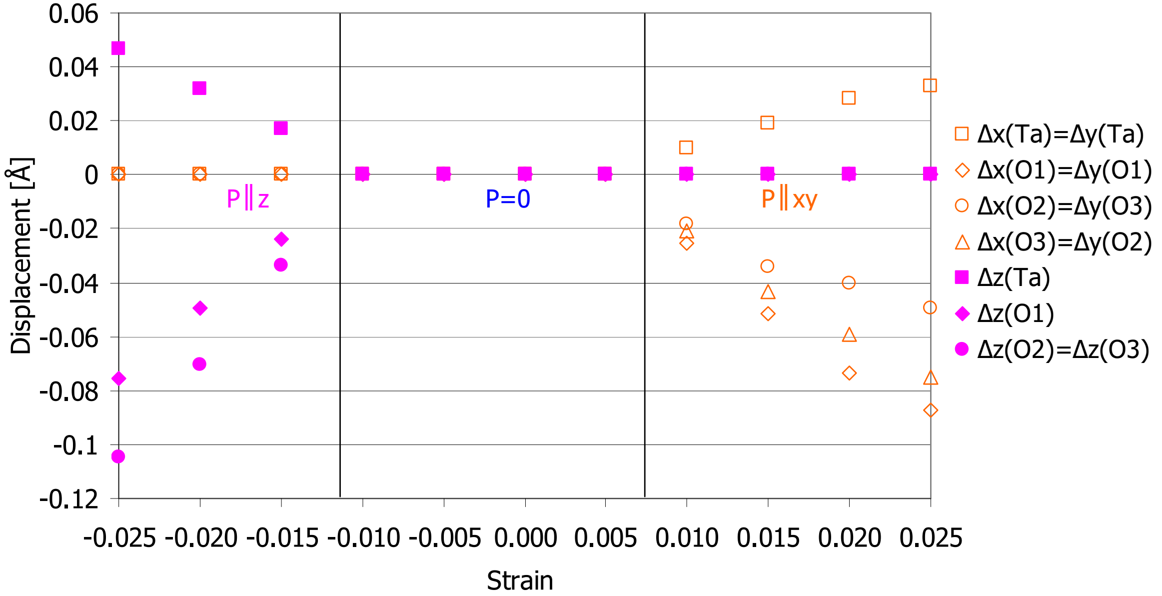

Displacements in strained $KTaO_3$

[4] M. Tyunina, J. Narkilahti, M. Plekh, R. Oja, R. M. Nieminen, A. Dejneka, and V. Trepakov, Phys. Rev. Lett. (in press)

Current studies

- Using hybrid functionals (B1-WC) for correct estimate of displacements and bandgaps in ferroelectrics
- Calculating quantum transport (tunneling) through ferroelectric layer
  - Conductivity determined by layer thickness and perovskite-electrode interface properties
  - Polarization direction may affect electrical conductivity if the interfaces are different [5], [6].

[5] M. Ye. Zhuravlev et al., Appl. Phys. Lett. **95** 052902 (2009)
[6] V. Garcia et al., Nature **460** 81 (2009)

3 (b) Comparative Study of *n*-type Transparent Conductive Oxides: SnO_2, In_2O_3, ZnO

(Péter Ágoston, Karsten Albe, Martti Puska)

Transparent Conducting Oxides - properties

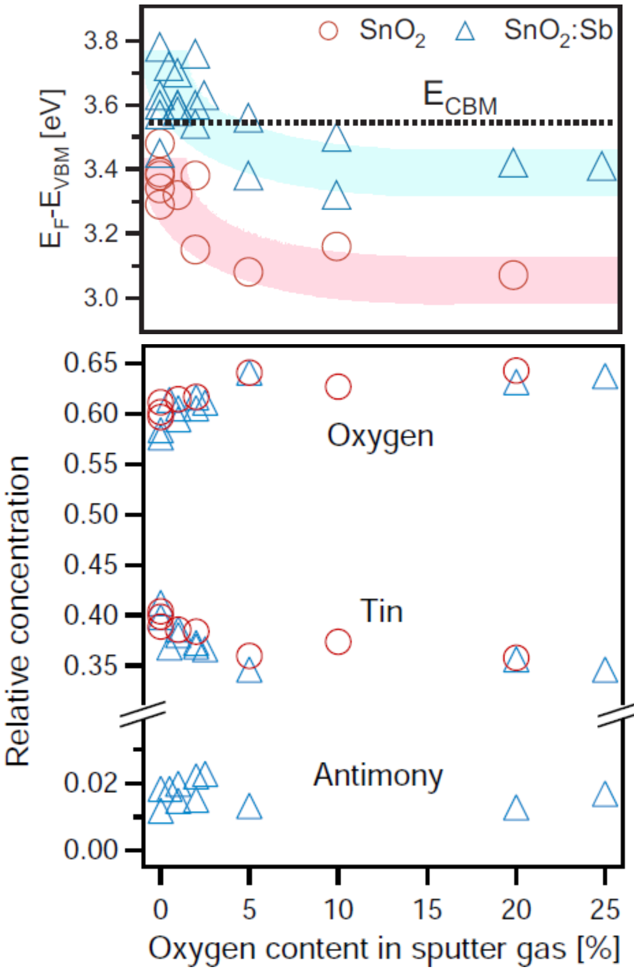

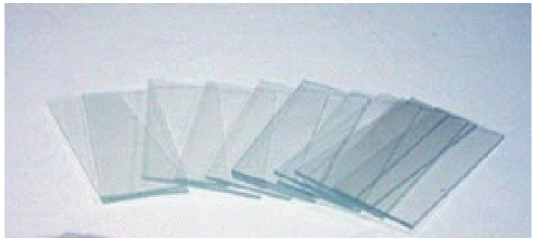

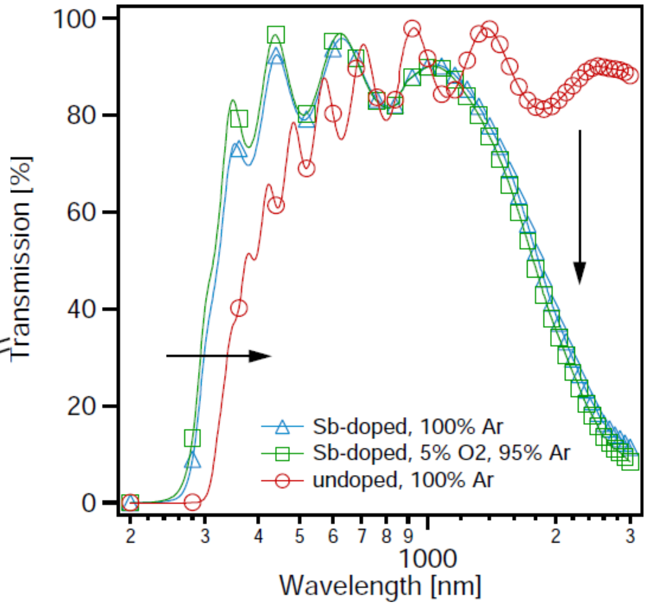

Key properties:

- *n*-type conductivity
- Non-stoichiometry
- Vis-Transparency

Typical Materials:

- ITO (In_2O_3:Sn)
- FTO (SnO_2:F)
- ATO (SnO_2:Sb)
- AZO (ZnO:Al)

C. Körber et. al. Sensors and Actuators B 139 2 665-672 (2009)

Transparent Conducting Oxides - applications

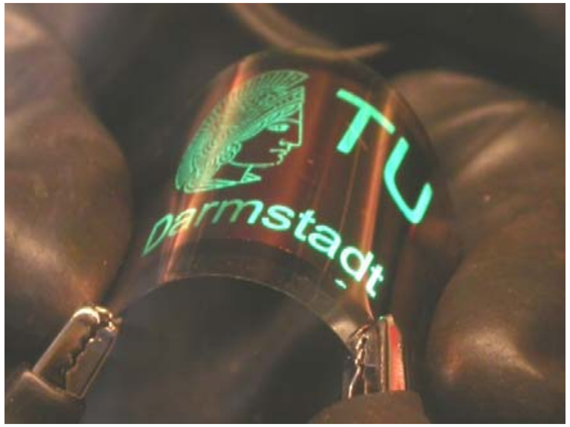

Organic LED

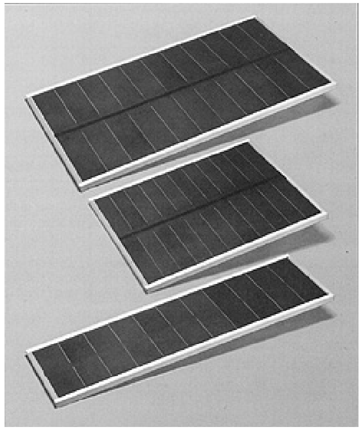

Thin film
Solar Cell

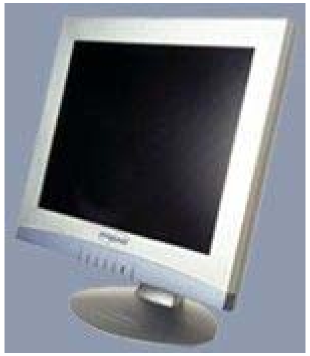

Flat Panel Display

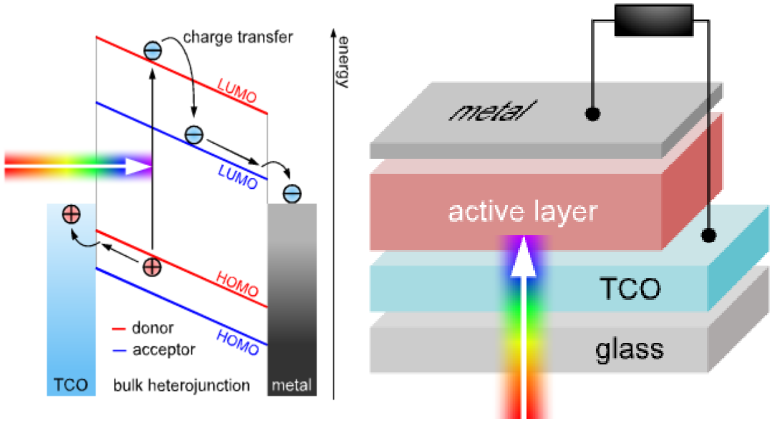

Organic solar cell

Gas Sensor

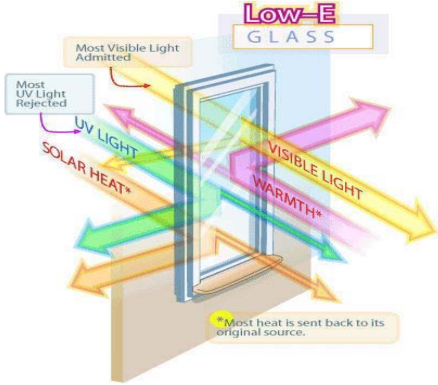

Low-e glass

Defect/impurity-related ionisation levels in insulators

“deep” donor

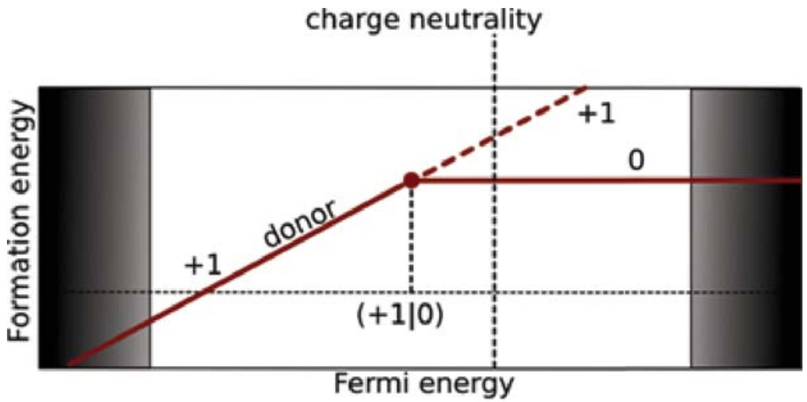

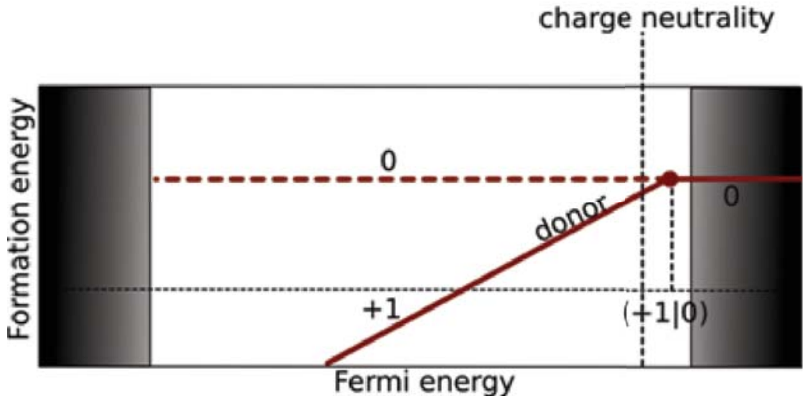

“shallow” donor

Possibilities for *n*-type TCO material

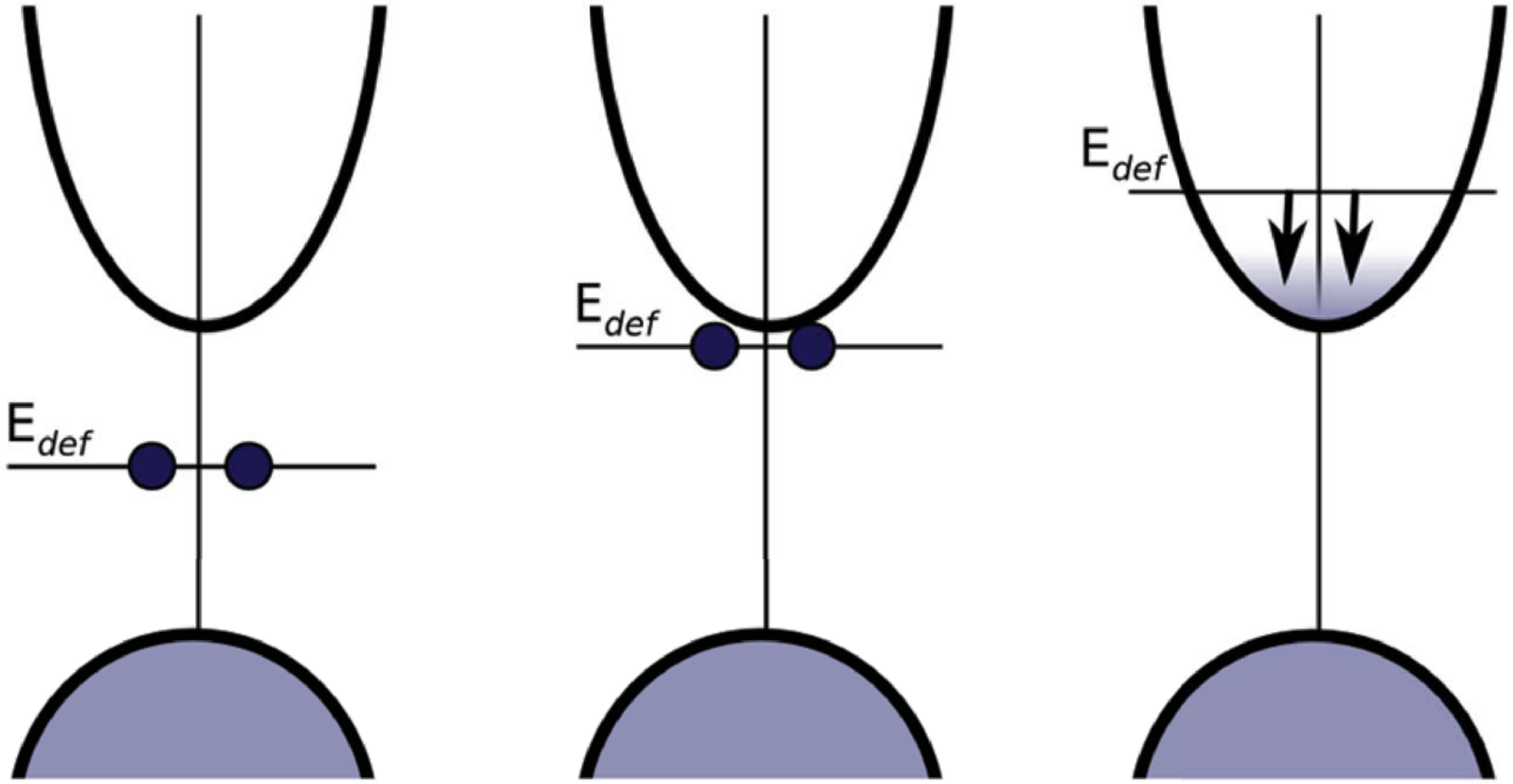

deep

shallow

resonant
effective mass like

Possibilities for *n*-type TCO material

Small band gap

- dopable
- not transparent

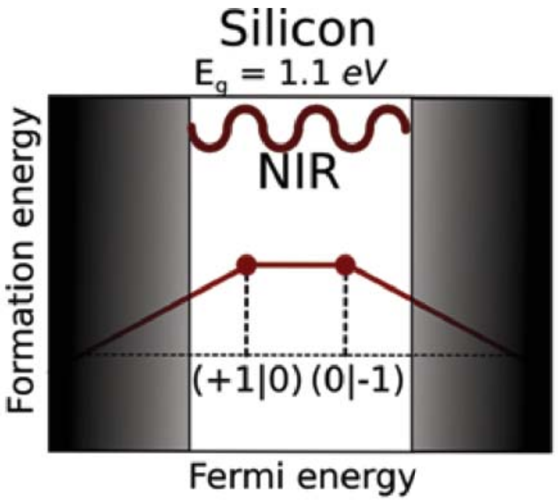

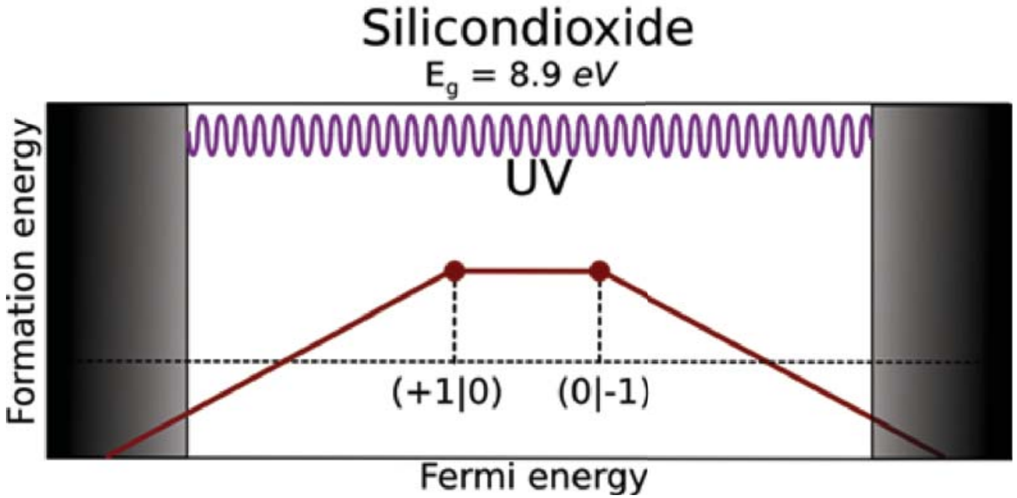

Large band gap

- not dopable
- transparent

n-type TCO materials

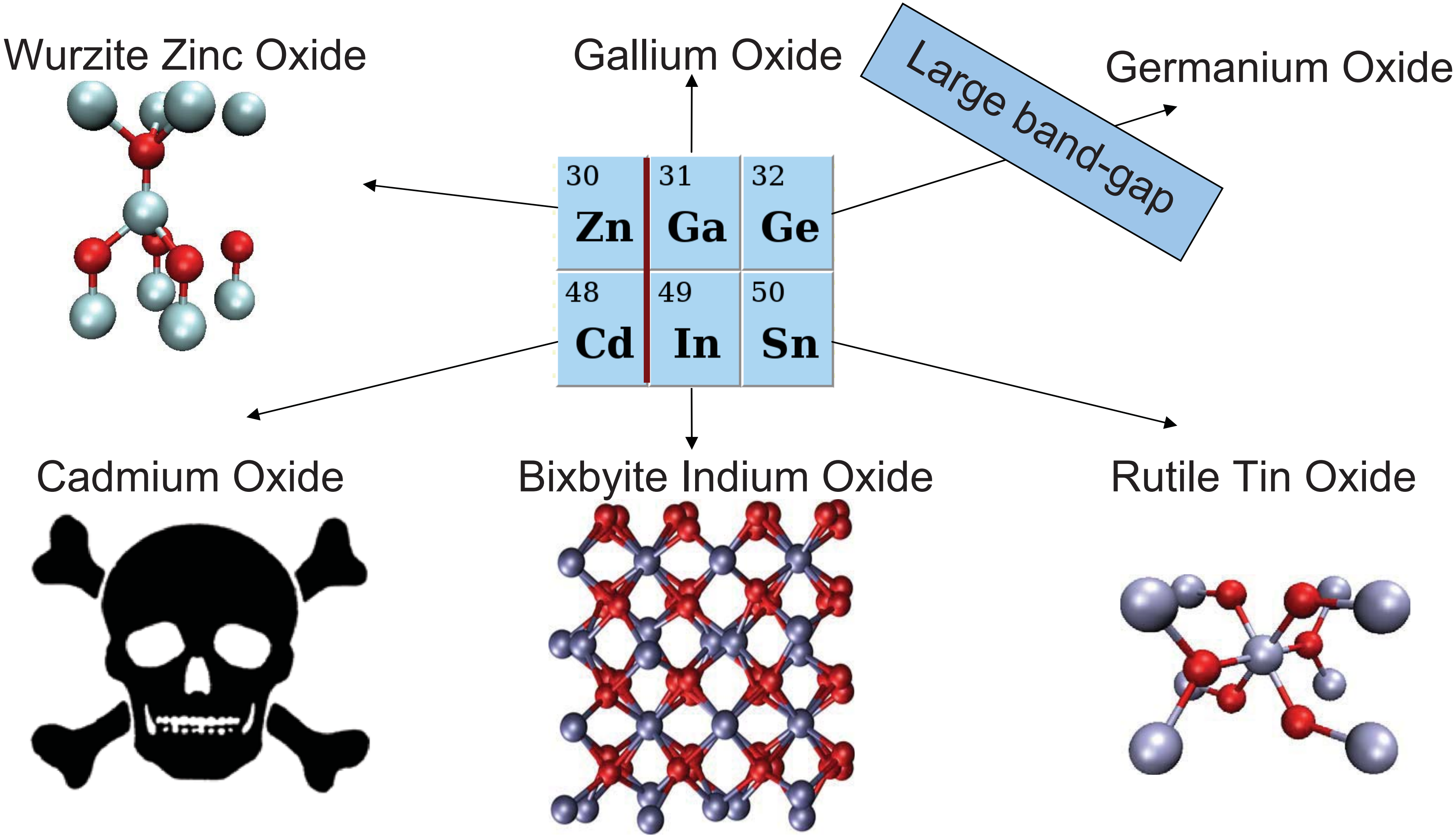

Wurzite Zinc Oxide

Gallium Oxide

Large band-gap

Germanium Oxide

30 **Zn**	31 **Ga**	32 **Ge**
48 **Cd**	49 **In**	50 **Sn**

Cadmium Oxide

Bixbyite Indium Oxide

Rutile Tin Oxide

Previous work

SnO_2

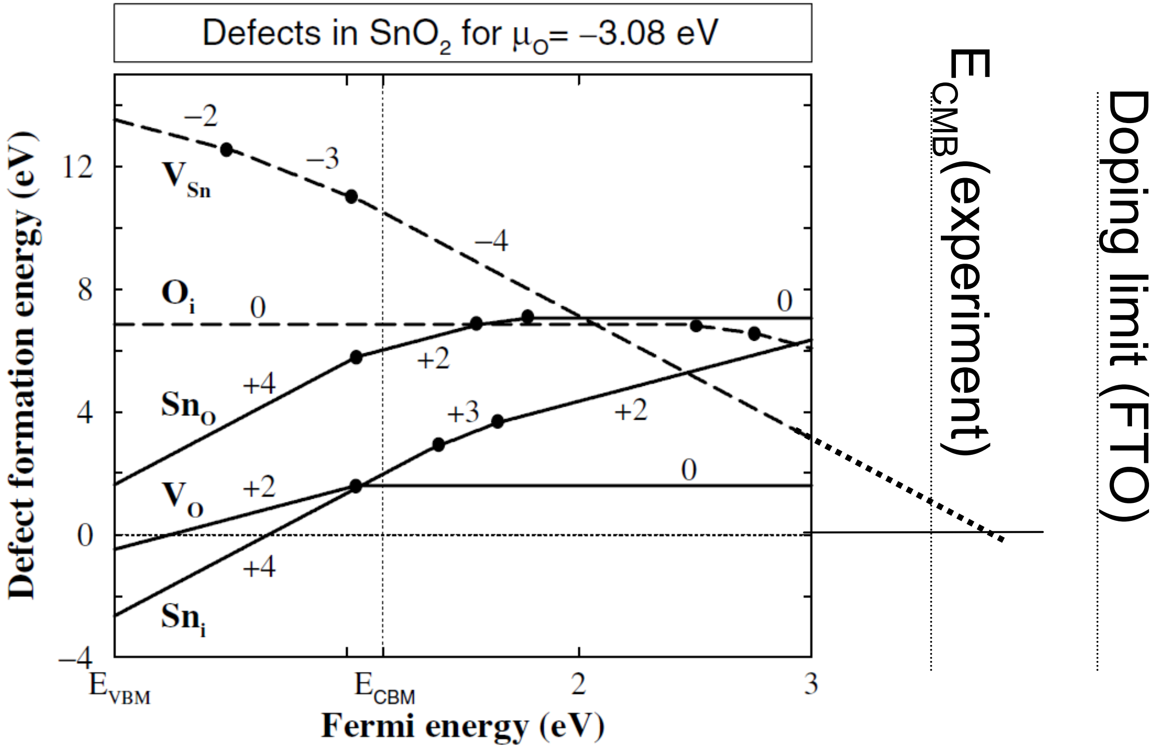

C. Kilic A. Zunger Phys. Rev. Lett. 88, 095501 (2002)

Previous work

- Persistent Photoconductivity (PPC)
- Similar behavior of ZnO and In_2O_3
- Explanation for *n*-type behavior

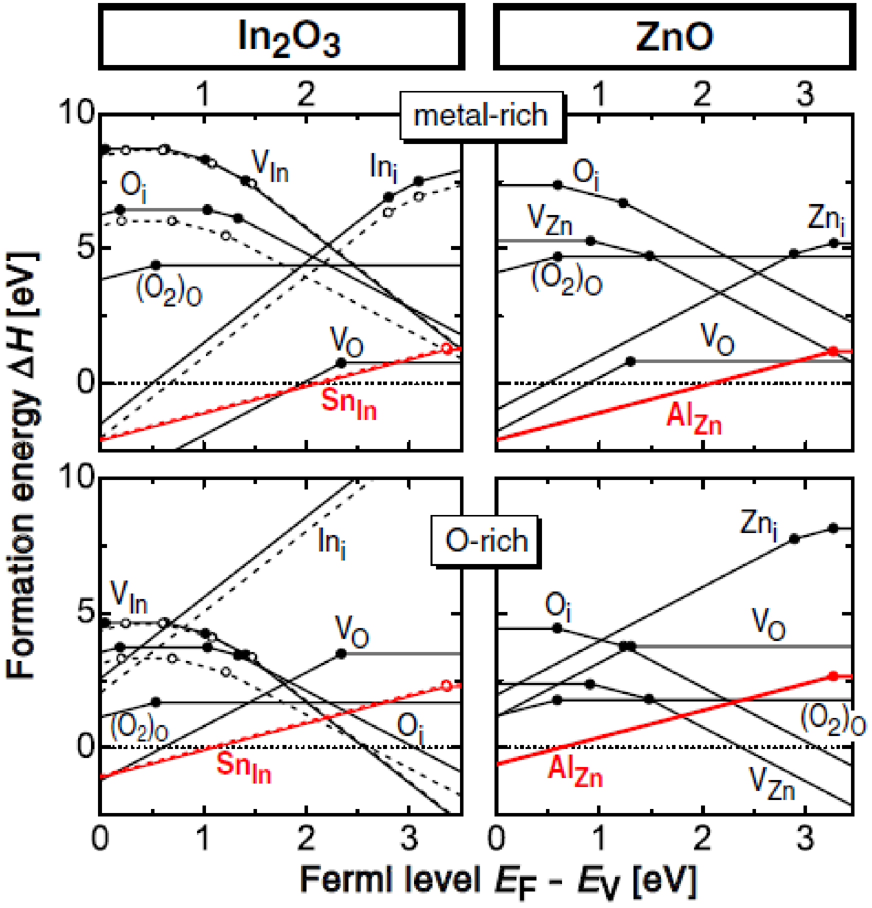

S. Lany & A. Zunger Phys. Rev. Lett. 98, 045501 (2007)

Previous work

SnO_2

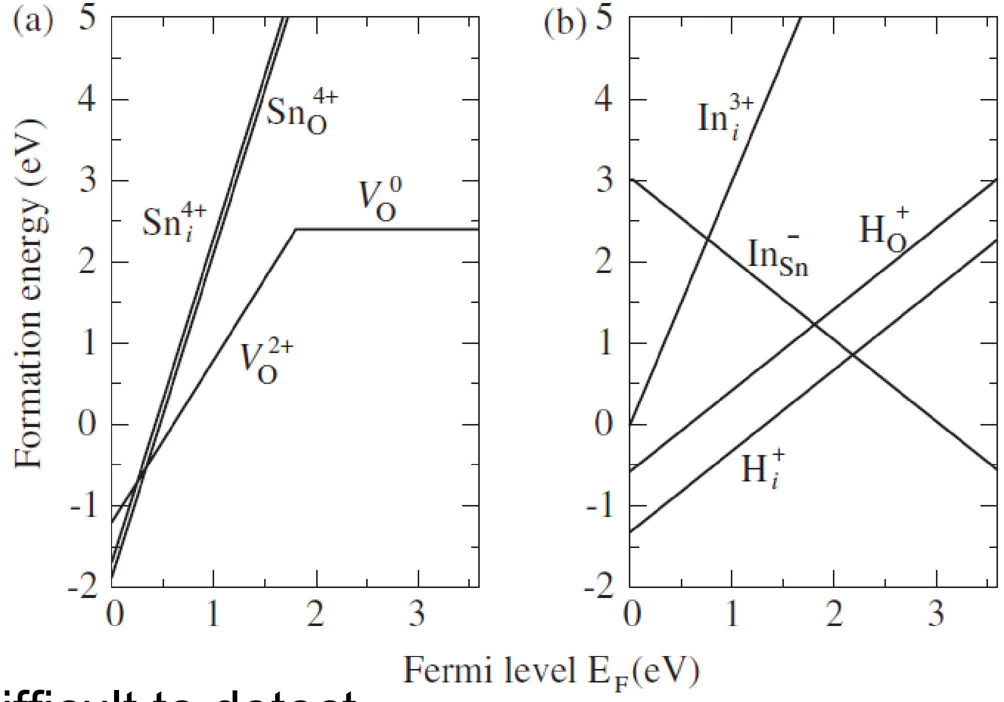

- Similar picture for SnO_2
- No *n*-type behavior
- Hydrogen as a donor
- Hydrogen is everywhere and difficult to detect

Singh et. al. Phys. Rev. Lett. 101, 055502 (2008)

Previous work: substitutional hydrogen

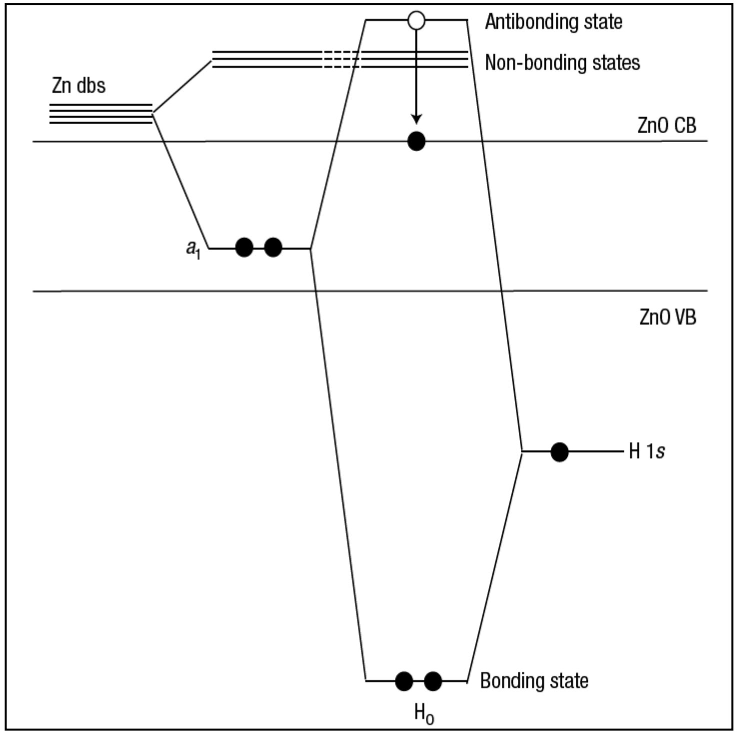

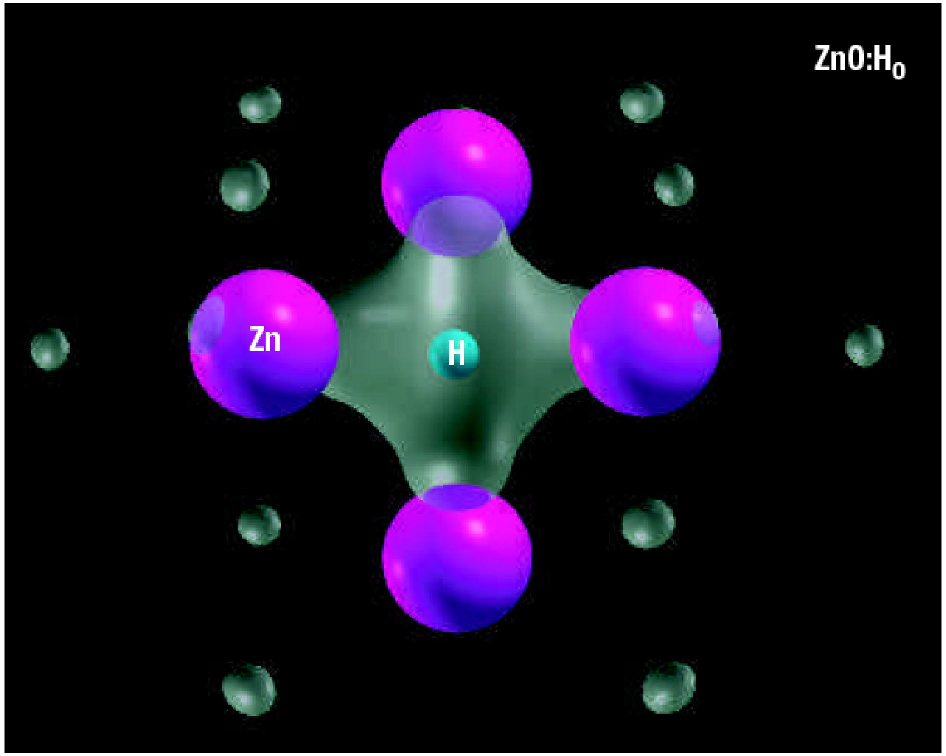

Janotti et. al. Nature Materials. 6, (2007)

LDA band gap problem

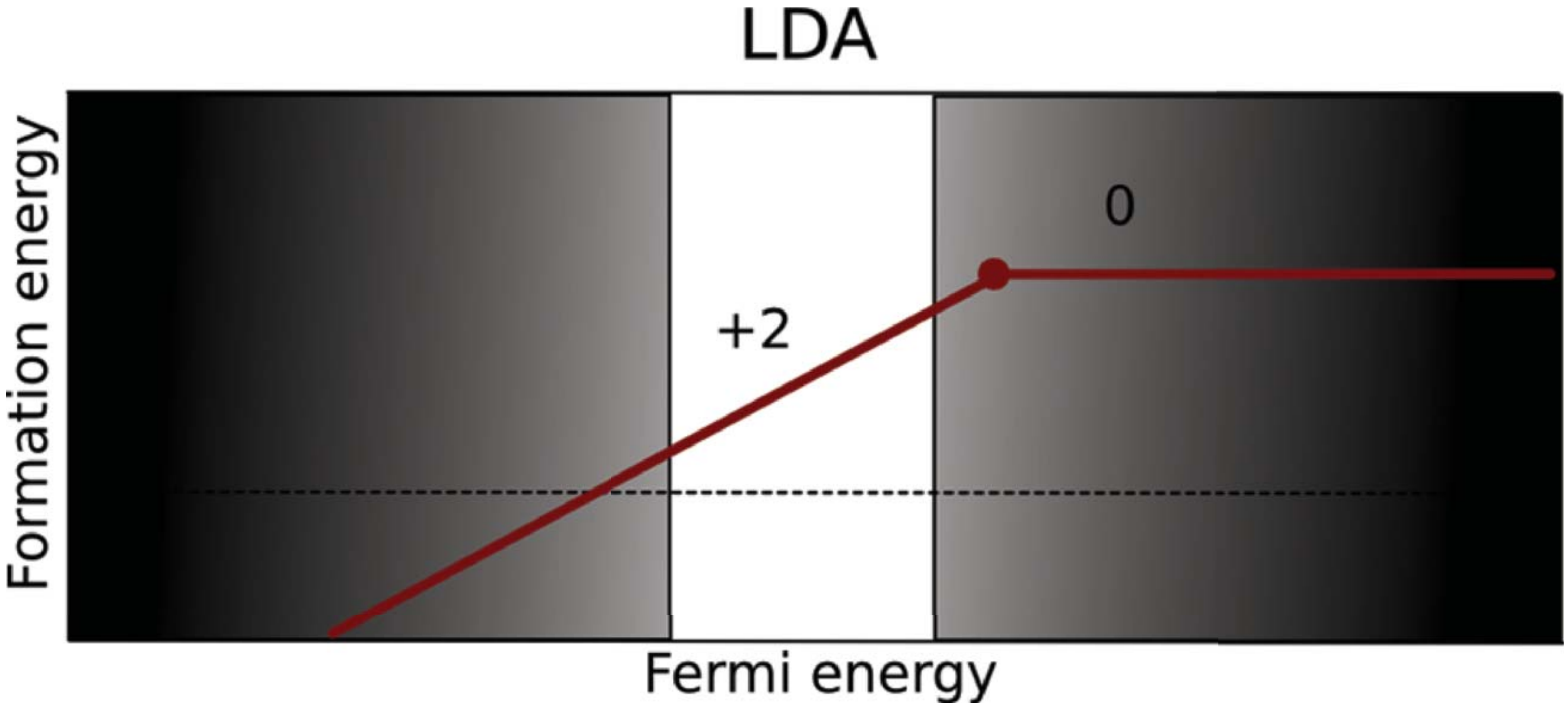

Defect states in LDA

Large gap insulator (alkali halides)

small gap insulator (TCO)

small gap semi-conductor (Ge,CIS)

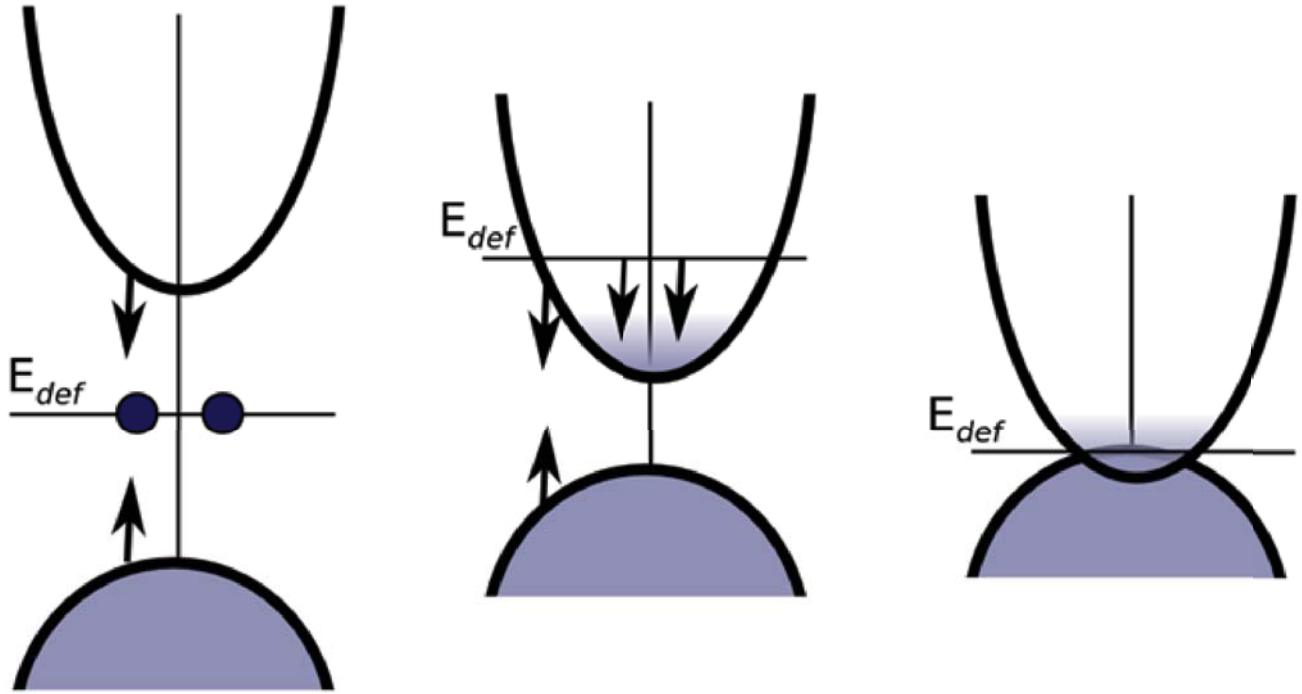

Motivation

- Conduction mechanism of TCO materials
- n- and p-type doping of TCO materials
- Role of stoichiometry
- Role of unwanted impurities

Very unsatisfactory from the theoretical point of view!

Native defects in TCOs: computational results

Effect of XC-functional

Inclusion of Hartree-Fock exchange into the XC-functional

→ Hybrid Functionals

PBE0
HSE06
B3LYP

Hartree-Fock exchange is really non-local!

Methodology: Density Functional Theory

Vienna ab-initio simulation package (Vasp)

- basis set : plane wave / periodic boundaries
- ion cores : projector augmented wave (PAW)
- V^{XC} : HSE06, PBE0, GGA+(*U*), LDA, GGA
- *U*-*J* : 7.0 (In_2O_3), 3.6 (SnO_2), 4.1 (ZnO)
- ***k***-points : 2 x 2 x 2 MP grid (Gamma only for HF-XC)
- E_{cut} : 500 eV
- cell sizes : 72(-750), 80(-640)

Intrinsic conductivity of *n*-type TCOs: role oxygen vacancies

Agoston *et al*. Phys. Rev. Lett. 103, 245501 (2009)

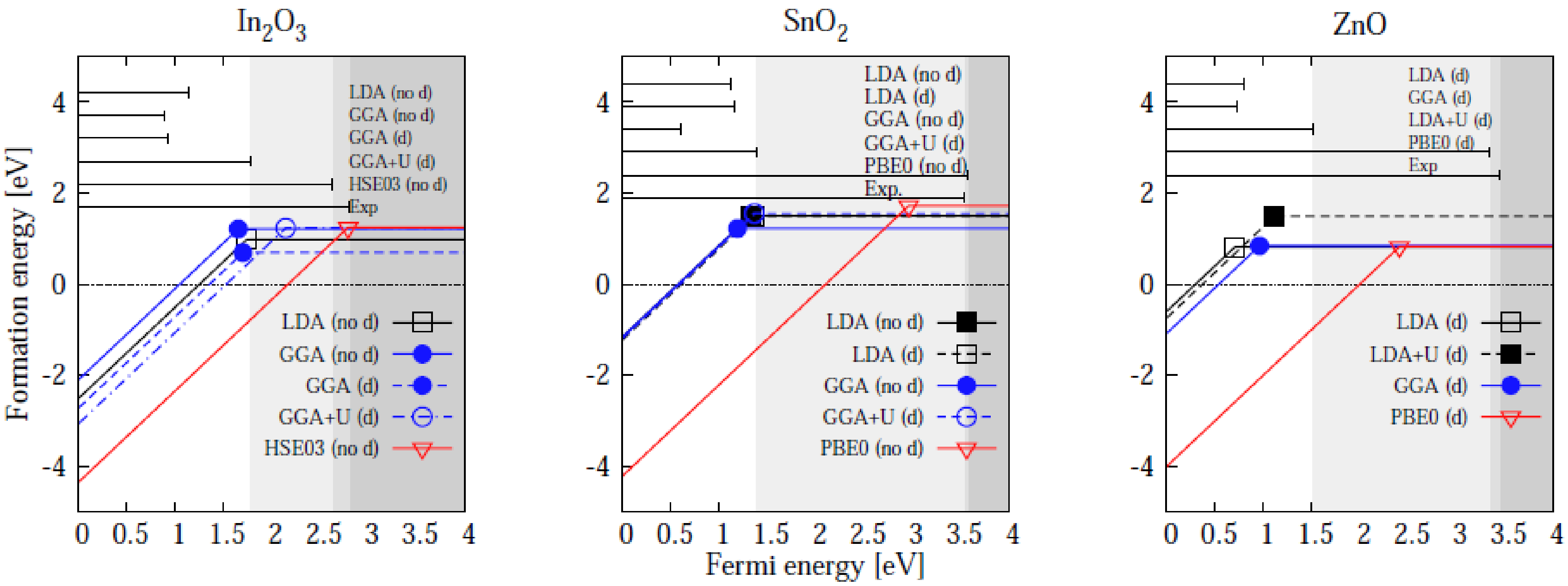

- Constant formation energies for the neutral charge state
- Strongly reduced formation energies for doubly positive charge states

Intrinsic conductivity of *n*-type TCOs

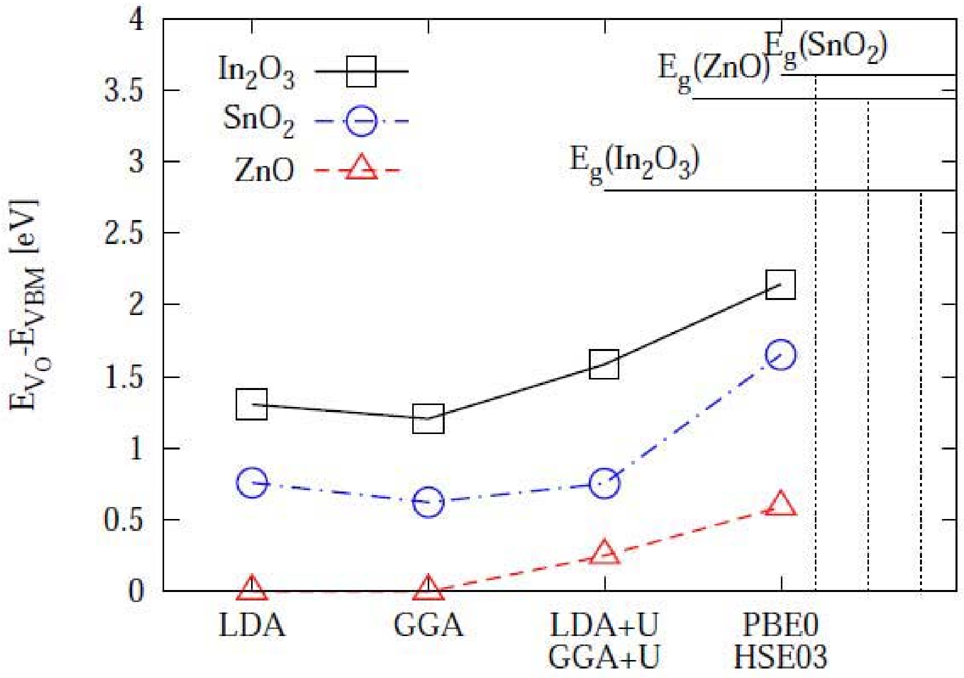

- Defect states shift upwards with increasing complexity of XC-functional
- Defects remain mainly deep donors

Acceptor defects: compensation

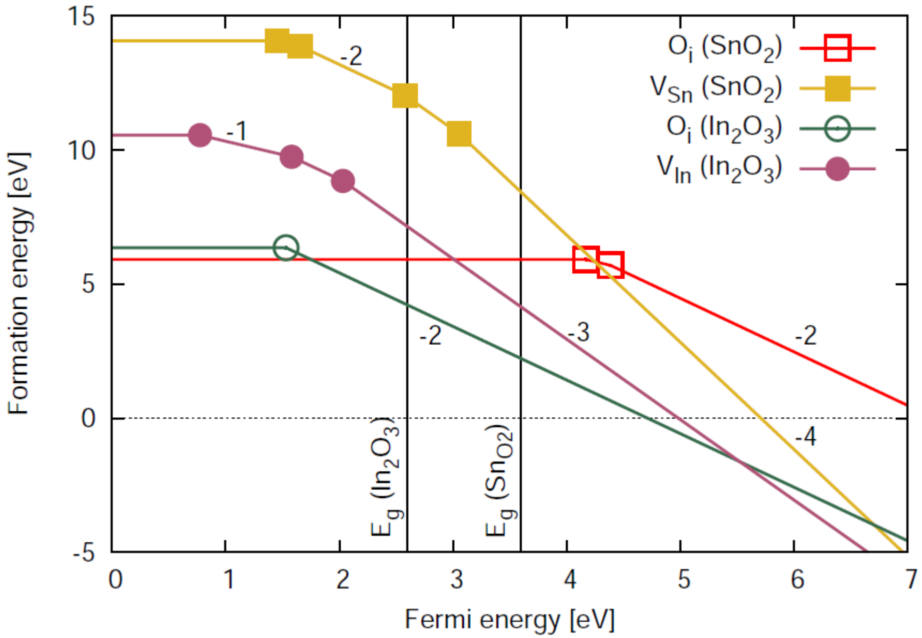

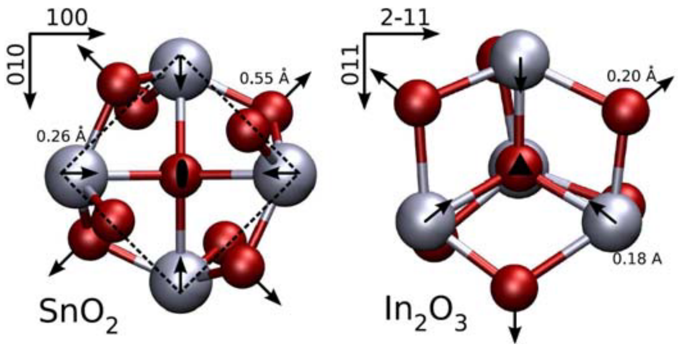

- Stability of acceptor defects increases with increasing Fermi energy
- High formation energies for acceptor defects
- The materials are now highly n-type dopable which is not the case in LDA

Acceptor defects

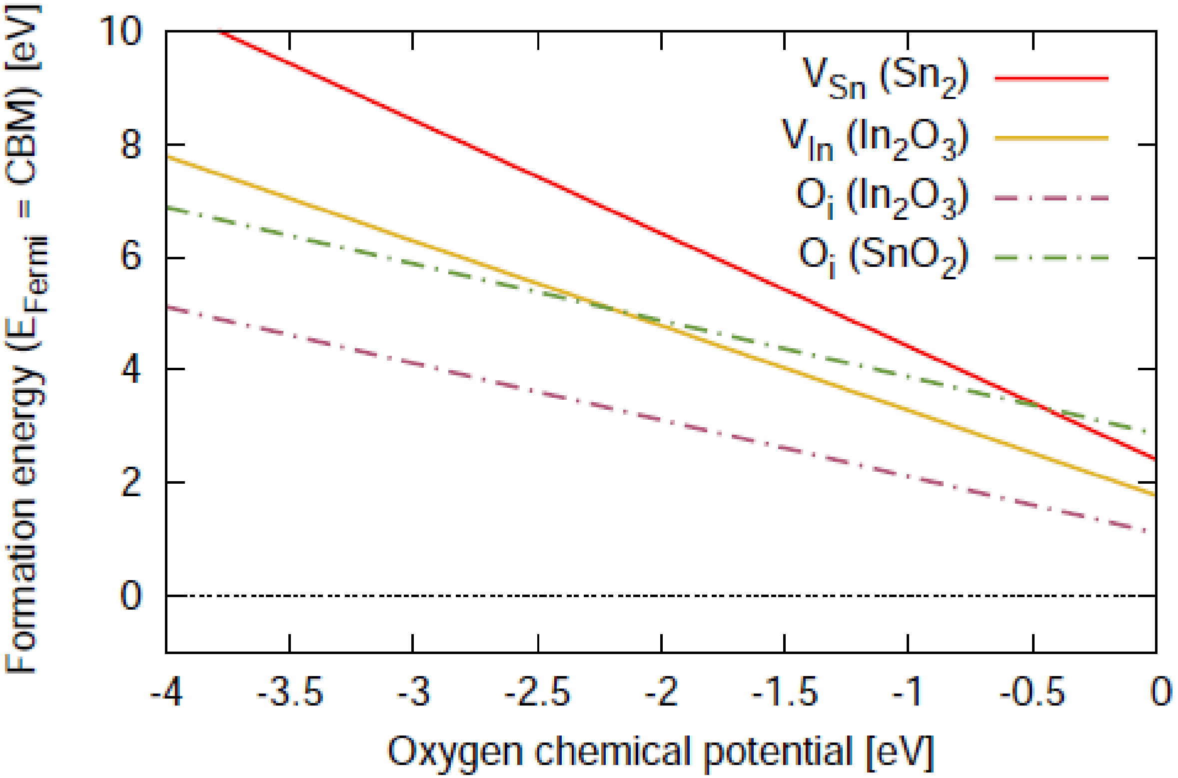

- Doping limits agree with experiment for In_2O_3 but not for SnO_2
- New doping strategies for SnO_2

Vacancy relaxation in *n*-type TCOs

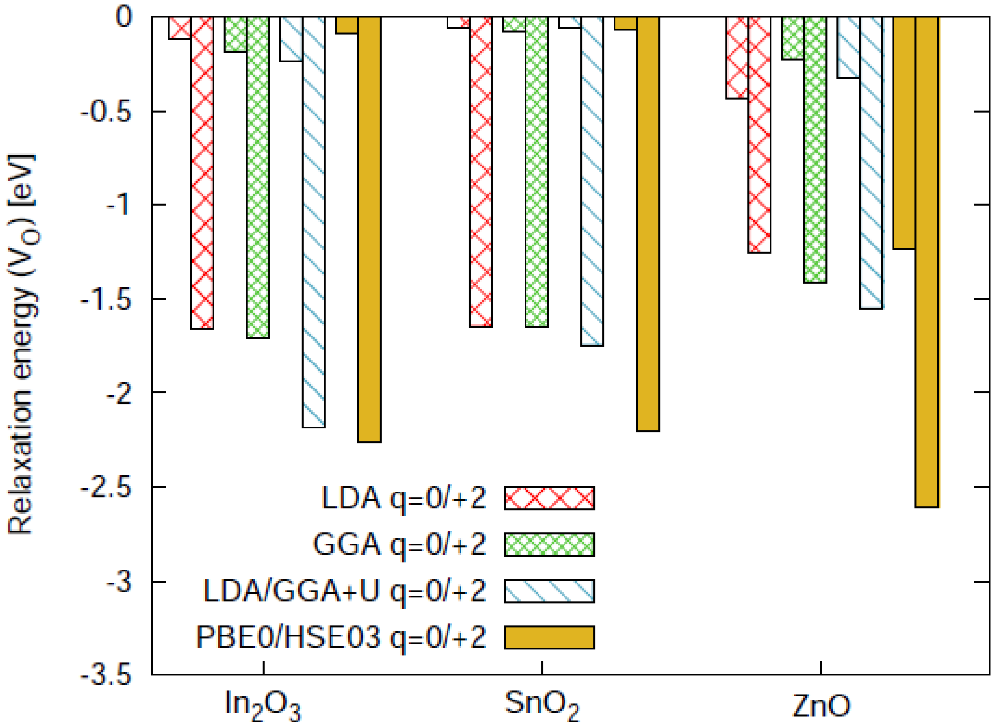

- Relaxation energy increase with the complexity of XC-functional
- Relaxation in neutral charge state only for ZnO

Cell size dependent defect state position: finite-size scaling for charged defects

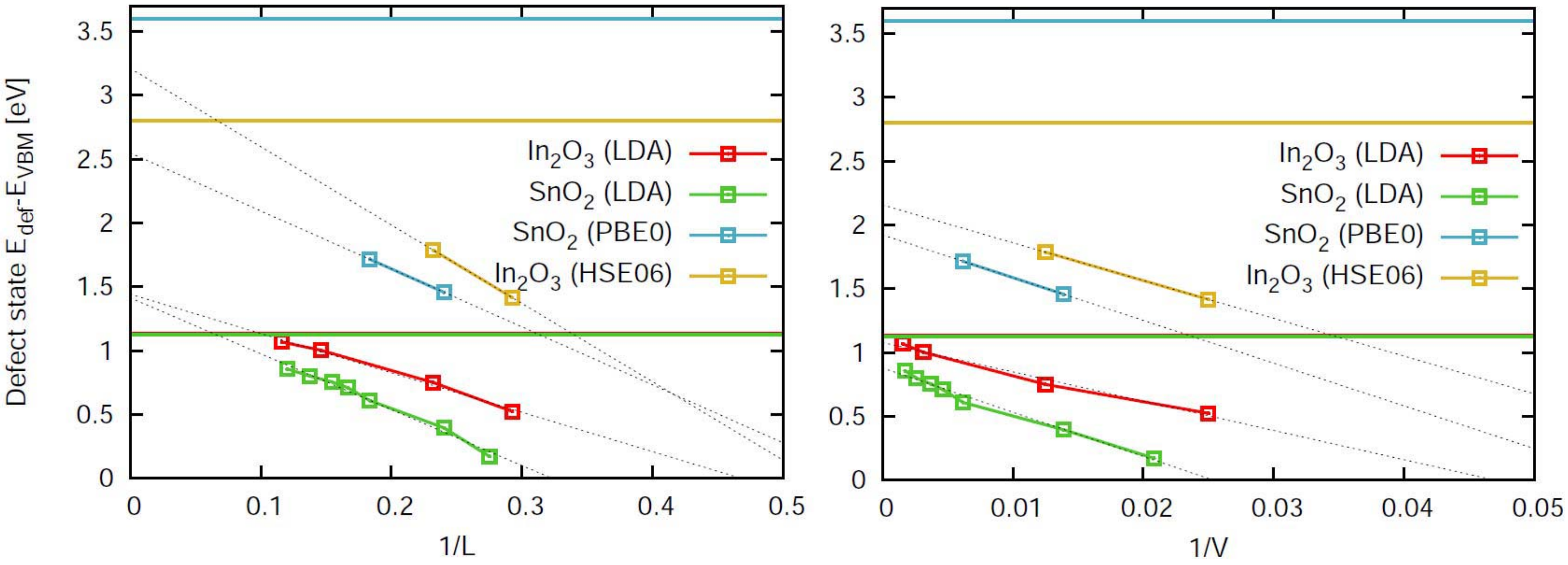

Summary and conclusions

- Hybrid functionals increase the *n*-type propensity for TCOs
- The effect is due to the underestimated bandgap, ionization potential
- The relaxation energies are not well described in LDA/GGA
- LDA/GGA + U is not the way to describe these materials
- Oxygen vacancies are shallow donor defects in In_2O_3
- Oxygen vacancies are moderately shallow in SnO_2
- Probably, additional contributions to *n*-type conductivity in SnO_2, ZnO
- Other (deep) donors in ZnO (H, PPC) cannot be excluded